Aus der Klinik für Hals-Nasen-Ohrenheilkunde und

der Klinik für Gynäkologie mit Schwerpunkt gynäkologische Onkologie

der Medizinischen Fakultät Charité-Universitätsmedizin Berlin

DISSERTATION

ALDH1-positive cancer stem-like cells enrich in nodal metastases of oropharyngeal squamous cell carcinoma independently of HPV-status

Zur Erlangung des akademischen Grades
Doctor medicinae (Dr. med.)

vorgelegt der Medizinischen Fakultät
Charité - Universitätsmedizin Berlin

von

Xu Qian
aus Zhejiang, China

Datum der Promotion: 25.10.2013

CONTENTS

LIST OF TABLES

LIST OF FIGURES

ABBREVIATIONS AND ACRONYMS

HNSCC	Head and neck squamous cell carcinoma
OSCC	Oropharyngeal squamous cell carcinoma
SCC	Squamous cell carcinoma
HPV	Human papillomavirus
HR-HPV	High risk-human papillomavirus
DNA	Deoxyribonucleic acid
T	Tumor size
N	Lymph node(s) involvement
M	Distant metastasis
c	Clinical
p	Pathological
r	Recurrences
G	Histopathological grade
LNs	Lymph nodes
RCT	Radiochemotherapy
CSC	Cancer stem (-like) cells
ALDH1	Aldehyde dehydrogenase isoform 1
p16^{INK4a}	p16 inhibitor of cyclin-dependent kinase 4a
CD	Cluster of differentiation
EMT	Epithelial-mesenchymal transition
DEAB	Diethylaminobenzaldehyde
HE-stain	Hematoxylin and eosin stain
IHC	Immunohistochemistry
FEPE tissue	Formalin-fixed paraffin-embedded tissue
HRP	Horseradish peroxidase
DAB	3,3-diaminobenzidine
ddH$_2$O	Double-distilled water
PBS	Phosphate-buffered saline
TBS	Tris-buffered saline
EDTA	Ethylene diamine tetraacetic acid
DMSO	Dimethyl sulfoxide

HCl	Hydrochloric acid
RT-PCR	Real time-Polymerase chain reaction
°C	Grad Celsius
μg	Microgram
μl	Microliter
mg	Milligram
ml	Milliliter
min	Minutes
RT	Room temperature

SUMMARY

Despite intensive efforts to improve the treatment of oropharyngeal squamous cell carcinoma (OSCC), the overall prognosis remains unsatisfyingly poor due to therapy resistance, loco-regional recurrence and metastasis. A small population of cancer cells, known as cancer stem (-like) cells (CSC) exhibiting a stem cell phenotype, is thought to drive malignancies and to be responsible for therapy resistance, recurrence and metastasis. Aldehyde dehydrogenase 1 (ALDH1), which has been intensively investigated in the carcinogenesis of head and neck cancer, is a confirmed marker for CSC of OSCC. A subgroup of OSCC is caused by infection with high-risk (HR) human papillomavirus (HPV) in 30–40% of all cases in Germany. HPV-positive and HPV-negative OSCC present different etiological entities with alternative mechanisms for carcinogenesis and different clinical features. It has been shown that HPV-positive OSCC affect a younger patient population with relatively little comorbidity. Therefore, sustainable therapeutic results with few long-term side effects are highly desirable.

The purpose of this study was to investigate associations between HR-HPV/p16^{INK4a} positivity, CSC-frequency, and clinico-pathological parameters in patients with metastatic OSCC.

HPV genotypes and expression of ALDH1 and p16^{INK4a} was analyzed in 40 paired OSCC primary tumors and matched metastases.

There was no association between HR-HPV with histological grade and tumor stage according to the TNM-classification in OSCC patients. A significant correlation of ALDH1 positivity with lower primary tumor differentiation grade (p=0.009) and higher nodal status (p=0.015) was noted. Compared to primary tumors, the proportion of ALDH1-expressing cells was significantly increased in metastases (p=0.012). While significantly less ALDH1-expressing cells were found in HR-HPV-DNA^{+}/p16$^{INK4a\ +}$ primary tumors (p=0.038) as compared to HR-HPV-DNA^{-}/p16$^{INK4a\ -}$ primary tumors, metastases showed no difference.

In conclusion, HPV^{+} and ALDH1^{+} CSC are detectable in OSCC and its corresponding metastases. OSCC with higher numbers of ALDH1-positive cells exhibit a more aggressive phenotype characterized by higher nodal classification and lower differentiation. This suggests a subpopulation contained in the ALDH1-positive OSCC cell pool able to complete the metastatic cascade and subsequently enrich in metastasis independently of tumor etiology and ALDH1 content.

ZUSAMMENFASSUNG

Trotz intensiver Anstrengungen die Behandlung von Oropharynxkarzinomen (OSCC) zu verbessern, ist die Gesamtprognose aufgrund von Therapieresistenz, lokoregionaler Rezidivierung und Metastasierung schlecht. Eine kleine Population von Tumorzellen mit Stammzellphänotyp, die als Tumorstammzellen (CSC) bezeichnet werden, wird für den neoplastischen Prozess und Therapieresistenz, Rezidivbildung und Metastasierung verantwortlich gemacht.

Das Enzym Aldehyddehydrogenase 1 (ALDH1) wurde umfassend im Zusammenhang mit der Karzinogenese von Kopf-Hals-Karzinomen untersucht und ist ein nachgewiesener Biomarker für Tumorstammzellen in OSCC. In 30-40% aller Fälle in Deutschland sind in OSCC Infektion mit Hochrisiko-(HR) Humanen Papillomviren (HPV) nachweisbar. HPV-positive und HPV-negative OSCC stellen unterschiedliche ethiologische Entitäten mit unterschiedlichen Mechanismen der Karzinogenese und klinischen Eigenschaften dar. Es konnte gezeigt werden, dass HPV-positive OSCC bei einer jüngeren Patientenpopulation mit relativ geringer Komorbidität vorkommen.

Deshalb sind anhaltende therapeutische Resultate mit geringen Langzeit-Nebenwirkungen höchst wünschenswert.

Das Ziel dieser Arbeit war es, Assoziationen zwischen HR-HPV/p16^{INK4a}–Positivität, CSC-Frequenz und klinisch-pathologischen Parametern von Patienten mit metastasiertem OSCC zu untersuchen.

HPV-Genotypenprävalenz und Expression von ALDH1 und p16^{INK4a} wurde in 40 zusammengehörigen OSCC-Primärtumoren- und Metastasen-Paaren untersucht. Es zeigte sich keine Assoziation zwischen HR-HPV mit histologischem Grad und TNM-Tumorstadium. Eine signifikante Korrelation von ALDH1-Positivität im Primärtumor mit niedrigerer Tumordifferenzierung (p=0,009) und höherem nodalem Status (p=0,015) wurde beobachtet. Im Vergleich zu Primärtumoren war der Anteil ALDH1-exprimierender Zellen in Metastasen statistisch signifikant erhöht (p=0,012). Während in HR-HPV-DNA^{+}/p16^{INK4a}-positiven Primärtumoren im Vergleich zu HR-HPV-DNA^{-}/p16^{INK4a}–negativen Primärtumoren signifikant weniger ALDH1-exprimierende Zellen gefunden wurden (p=0,038), zeigte sich in Metastasen kein Unterschied.

Zusammenfassend sind HPV- und ALDH1-positive CSC in OSCC und den jeweils korrespondierenden Metastasen nachweisbar. OSCC mit hohen Zahlen an ALDH1-positiven Zellen zeigen einen aggressiveren Phänotyp, der durch eine höhere nodale Klassifikation und niedrigere Differenzierung charakterisiert wird. Dies suggeriert eine, im ALDH1-positiven

OSCC-Zellpool enthaltene Subpopulation, die in der Lage ist, die metastatische Kaskade zu komplettieren und nachfolgend in Metastasen, unabhängig von der ursprünglichen Tumorethiologie und des ALDH1-Gehalts, nachweisbar ist.

1 Introduction

1.1 Oropharyngeal squamous cell carcinoma (OSCC)

1.1.1 Definition of OSCC

Squamous cell carcinoma arising from oropharynx, which includes the base-of-the tongue, the tonsils, the soft palate, and the side and back wall of the throat, is a subtype of head neck squamous cell carcinoma (HNSCC). In OSCC, the most commonly affected sites are the base-of-tongue and the tonsils accounting for 90% of all OSCC [50].

1.1.2 Epidemiology and risk factors

OSCC is one of the most prevalent and lethal cancers worldwide [50]. Tobacco use and alcohol consumption are the main risk factors for the development of OSCC. In recent years, much attention has been paid to the possible role of human papillomavirus (HPV) infection in the pathogenesis of OSCC [50]. HPV association has been detected in about 30-40% of OSCC in Germany, and 40-80% in USA [14, 61,71].

Over the past 20 years, the incidence of OSCC displays a sharp increase in contrast to other head and neck cancers. Many attribute this to a rise especially in high-risk-(HR-) HPV-related OSCC while the incidence of HR-HPV-unrelated OSCC steadily decreases with reduced alcohol and tobacco abuse (Figure 1.1) [14,54,66].

A recent meta-analysis reported that overall HPV prevalence in OSCC increased significantly over time: from 40.5% before 2000, to 64.3% between 2000 and 2004, and 72.2% between 2005 and 2009. HPV rather than tobacco and alcohol has been the major cause of OSCC in Western-Europe and North-America [62]. Therefore, a subgroup of OSCC initially caused by infection with HR-HPV has been defined.
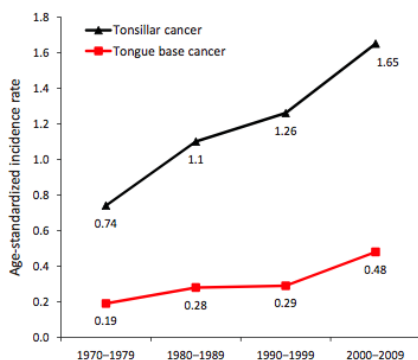
1.1.3 Histological and TNM classification and staging system of OSCC

Squamous cell carcinoma (SCC) is a malignant epithelial tumor, which originates from the squamous epithelium or ciliated respiratory epithelium. Histologically, squamous cell carcinoma is characterized by invasive growth and squamous differentiation. Invasive growth is characterized by interruption of the basal membrane and the growth of islands, cords, or single tumor cells in the stroma or deeper invasion into muscle, cartilage and bone. Squamous differentiation is defined by intercellular bridges and/or keratinisation, with keratin pearl formation. OSCC can be classified by its histological type as applied in daily clinical routine. SCC are commonly graded into GX, grade cannot be assessed; G1, well-differentiated; G2, moderately differentiated; G3, poorly differentiated; and G4, undifferentiated (Figure 1.2) [6]. Beside the histological grade, the TNM classification and staging system as illustrated in tables 1.1 and 1.2 is also important instruments for prognostic evaluation and therapy-planning. The T-stage describes the size of the primary tumor and invasion of other regions or organs, the N-stage describes the size and number of involved regional (cervical) lymph nodes (LNs) and the M-stage describes the status of metastases. The prefix "c" is used to describe clinical- and the prefix "p" for pathological assessments. The prefix "r" is used for recurrences.
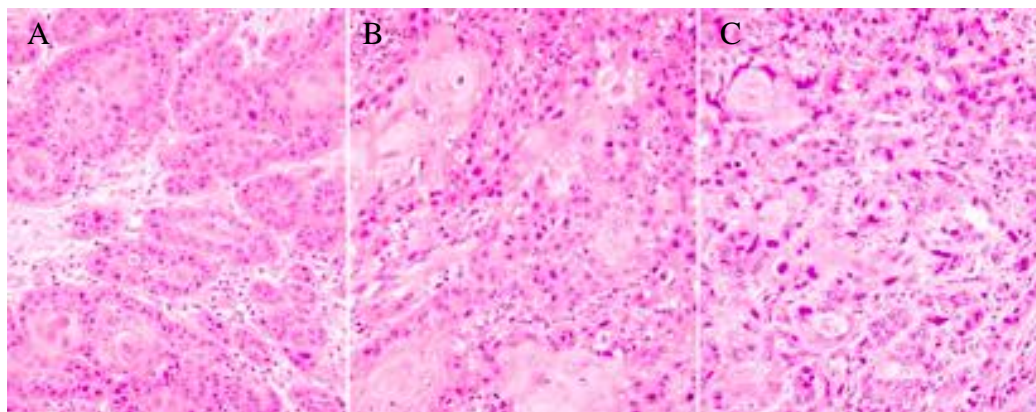
Figure 1.2 Histological grading of OSCC. (A) Well-differentiated squamous cell carcinoma. (B) Moderately differentiated squamous cell carcinoma. (C) Poorly differentiated squamous cell carcinoma [6].

Table 1.1 The TNM classification of OSCC [27].

T= size of primary tumor	
Tx	Cannot be assessed
T0	No evidence of primary tumor
Tis	Carcinoma in situ
T1	Tumor ≤ 2 cm in greatest dimension
T2	Tumor > 2 cm to 4 cm in greatest dimension
T3	Tumor > 4 cm in greatest dimension or extension to lingual surface of epiglottis
T4a	Moderately advanced local disease. Tumor invades the larynx, deep/extrinsic muscle of tongue, medial pterygoid, hard palate, or mandible
T4b	Very advanced local disease. Tumor invades lateral pterygoid muscle, pterygoid plates, lateral nasopharynx, or skull base, or encases carotid artery.
N= metastatic involvement of regional lymph nodes	
Nx	Regional lymph nodes cannot be assessed
N0	No regional lymph node metastasis
N1	Metastasis in a single ipsilateral lymph node, ≤3 cm in greatest dimension
N2	Metastasis in a single ipsilateral lymph node, >3 cm but ≤6 cm in greatest dimension, or metastasis in multiple ipsilateral lymph nodes, ≤6 cm in greatest dimension, or in bilateral or contralateral lymph nodes, ≤6 cm in greatest dimension.
N2a	Metastasis in a single ipsilateral lymph node >3 cm but ≤6 cm in greatest dimension
N2b	Metastasis in multiple ipsilateral lymph nodes, ≤6 cm in greatest dimension
N2c	Metastasis in bilateral or contralateral lymph nodes, ≤6 cm in greatest dimension
N3	Metastasis in a lymph node >6 cm in greatest dimension
M= presence of distant metastasis	
Mo	No distant metastasis
M1	Distant metastasis

Table 1.2 OSCC stage grouping according to the TNM classification of malignant tumors [27].

OSCC stage grouping			
Stage 0	Tis	N0	M0
Stage I	T1	N0	M0
Stage II	T2	N0	M0

Stage III	T3	N0	M0
	T1	N1	M0
	T2	N1	M0
	T3	N1	M0
Stage IVA	T4a	N0	M0
	T4a	N1	M0
	T1	N2	M0
	T2	N2	M0
	T3	N2	M0
	T4a	N2	M0
Stage IVB	T4b	Any N	M0
	Any T	N3	M0
Stage IVC	Any T	Any N	M1

1.2. Human papillomavirus (HPV) infection in OSCC

The role of HPV in carcinogenesis was first postulated by zur Hausen in 1976 in cancer of the cervix uteri and now has been widely explored in cancers including squamous cell carcinoma in the head and neck region, especially in the oropharynx [3,4,104].

1.2.1 Basics of HPV virology

HPV are small, strictly epitheliotropic viruses with a circular double-stranded DNA structure (Figure 1.3) that can infect stratified squamous cutaneous or mucosal epithelial cells (Figure 1.4) [2,86]. Papillomavirus genomes comprise 7,500-8,000 bp. The virus contains two main oncogenes, E6 and E7. More than 100 HPV genotypes are known to date. Epidemiologic studies and laboratory experiments establish a causal link between infections with HR-HPV types and the development of malignant tumors. Conversely, types found primarily in non-malignant lesions were labeled as 'low-risk' types [104]. 15 HR-HPV types (16, 18, 31, 33, 39, 45, 51, 52, 53, 56, 58, 59, 68, 73, and 82), putative HR-HPV (26, 35, 66) are confirmed carcinogens and several low-risk types (e.g. HPV 6, 11, 40, 43, 54, 71, 72, 74) contribute to non-invasive disease burden. Among them, HPV16 is acknowledged as the most carcinogenic HR-HPV type causing malignancies of the cervix, vulva, vagina, penis, anus, oral cavity, oropharynx and tonsil. The genome organization of HPV16 is shown in figure 1.5 [33]. Failure to clear HPV infection leaves host cells under the influence of the viral oncogenes. HPV-derived oncogenes are vital to the tumor cells survival and proliferation.
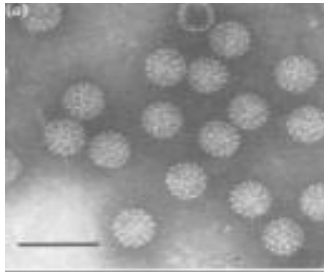
Figure 1.3 Electron micrograph of icosahedric papillomavirus particles [5]. Scale Bar: 1 μm.

HPV reaches the basal lamina through micro-injury that exposes the extra-cellular matrix

Infection of the basal cells, the epithelium's stem cell reservoir. Productive infection: production of virus particles in differentiating cells

Virus clearance within 8-18 months

Persistent infection: lasting > 18 months, transformation of cells by HPV integration in differentiated or basal (stem) cells

Cure

Offspring cells contain integrated HPV-DNA and upregulate expression of viral oncogenes (E6, E7)

Acquisition of further genetic changes leads to tumor progression

Figure 1.4 The HPV life cycle [2].

HPV reaches the basal epithelial layer through micro-injuries of the mucosa and binds to extracellular matrix components. Upon contact to cells of the epithelial basal cell compartment, that divide to regenerate the epithelium after injury, the virus infects these cells and may become quiescent together with the reacquired stem cell phenotype. This allows for prolonged persistence of viral infection and fixation of the infection in the epithelial stem cell. This may in part also be balanced by the viral oncogenes E6, E7, and the transcription repressor E2. When epithelial cells differentiate, the viral genetic program is switched and structural proteins are induced. During tumor progression integration of the viral genome into the host cell genome occurs at a random position.
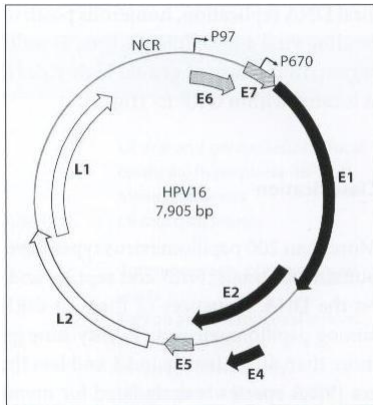
Figure 1.5 Organization of the circular, double-stranded DNA genome of HPV16. Open reading frames (ORFs), which encode proteins necessary for virus replication, transcription, and viral release, are depicted in black; genes, which encode proteins with oncogenic activity, in grey, and ORFs for structural proteins of the transcriptional promoters of early (E) (p97) and late (L) (p670) genes are indicated [33].

1.2.2 HPV-related and HPV-unrelated OSCC

Syrjanen *et al*. gave the first report of HPV infection in OSCC in 1983 [95]. HPV-DNA was first detected in OSCC in Germany in 1985 [23]. OSCC is now considered the second most common HPV-associated cancer. Figure 1.6 presents a typical HPV-positive tonsillar squamous cell carcinoma.
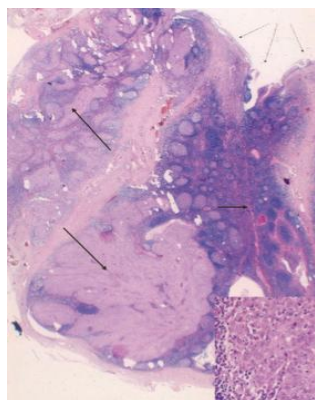
Figure 1.6 Typical HPV-positive tonsillar carcinoma (long arrows and insert) raised from the crypt epithelium (short arrow), whereas the tonsillar surface (thin arrows) does not show signs of malignant cell growth. The anatomic structure of the tonsils is characterized by tonsillar crypts that are lined with a monolayer epithelium similar to basal keratinocytes of mucosa [44].

From histological and clinical experience, HR-HPV-associated OSCC defines a distinct subgroup of the disease. Usually, patients affected by HPV-related or HPV-unrelated OSCC differ in incidence, age, genetic background, and prognosis (Table 1.3) [4,30,40,43]. HR-HPV-

related OSCC affects younger patients in contrast to alcohol- and tobacco-related OSCC. HPV-negative OSCC frequently carry a TP53 mutation while HPV-positive carcinomas carry wild-type TP53. Klussmann *et al.* identified the differences of chromosomal and genetic profiles in HPV16-related and -unrelated OSCC. The major conclusions of this study were: (1) higher number of chromosomal alterations and amplifications, more losses at 3q, 5q, 9p, 15q, and 18q, and gains/amplifications at 11q13, and fewer 16q loss and Xp gains were harbored in HPV-negative OSCC; (2) Interestingly, 16q losses, predominantly identified in HPV-related OSCC, was strongly indicative of a better overall survival and disease-free survival, and none of these patients had a tumor recurrence [43]. The lower rate of carcinogenic risk factors and p53 mutations and a younger patient population suggest that factors, currently unknown, are associated with viral entry, propagation/transformation, and immune evasion in HPV-related OSCC patients [2,50]. Therefore, with these two different etiologies, different treatment options according to the origin of the malignancies, being spontaneously or virally induced, may be developed to target the cancer efficiently. Importantly, patients with HPV-related tumors have a better outcome compared to patients with HPV-unrelated tumors after treatment. The treatment options may include surgery with adjuvant radiotherapy (RT) or radiochemotherapy (RCT) with or without induction chemotherapy (Table 1.4) [40] and are composed according to the disease status and possible patients' comorbidities. Routine examination of OSCC with HPV status is now recommended in United States guidelines [7] but currently not in Germany.

Table 1.3 Clinical differences between HPV-positive and HPV-negative OSCC [40].

HPV-positive tumors	HPV-negative tumors
Younger patient	Older patient
Nonsmoker	Smoker, alcohol user
Sexual risk factors	-
Good performance status	Bad performance status
Tonsil and base-of-tongue	All subsites
Nonkeratinized	Keratinized
Stage T1-2, N+	Stage T3-4, N variable
Increasing incidence	Decreasing incidence
Good prognosis	Bad prognosis

Table 1.4 2- and 5-year overall survival (OS) rates for HPV-related and HPV-unrelated OSCC after different treatment regimens [40].

	Treatment	2-year OS		5-year OS	
		%HPV^{+}	%HPV^{-}	%HPV^{+}	%HPV^{-}
Licitra *et al.* [53]	S + R(C)T	92	68	79	46
Reimers *et al.* [77]	different	73	65	73	49
Smith *et al.* [91]	different	83	68	76	58
Lassen *et al.* [48]	RT	86	51	62	26
Fakhry *et al.* [28]	IC + RCT	95	56	75	46
Settle *et al.* [87]	IC + RCT	90	50	86	31
Rischin *et al.* [78]	RCT	91	74	88[a]	68[a]
Ang *et al.* [4]	RCT	90	65	82[a]	57[a]

S = Surgery; IC = induction chemotherapy.

[a] 3-year OS.

1.2.3 Cervical lymph node metastasis of OSCC and HPV infection

Squamous cell carcinomas can spread directly to contiguous structures via lymphatic or blood vessels, to seed regional LNs and/or distant metastases. OSCC are very lymphophilic and have a high tendency to metastasize to the regional LNs. Cervical lymph node metastasis is regarded as an important prognostic factor in OSCC [24,96,100].

Cervical nodal metastasis was reported to be more frequent in HPV16-positive cancers [35]. A recent study demonstrated that HPV16 DNA detection in LNs of patients with OSCC is an indicative marker of metastasis [64]. Ang *et al.* showed that the nodal stage (N0 to N2a vs. N2b to N3) was the major determinant of overall survival in HPV-positive OSCC patients [4]. However, the interplay between the virus and lymphoid tissue, which may account for differences in the biology of the diseases and treatments, still has not been well documented.

1.3 Biomarkers of HPV infection in OSCC

Questions have arisen recently with regard to what the best prognostic biomarkers for HPV infection in OSCC are. The detection of active HPV infection can vary according to the different methods [84,90] including PCR-based detection of E6/E7 mRNA, or HPV-DNA detection illustrated as follows. In general, over-expression of p16^{INK4a} is used as a surrogate marker for HPV infection. Its expression can be tested by immunohistochemistry. It was reviewed by Lewis JS Jr. that p16^{INK4a} protein overexpression was sensitive for the presence of HPV and was strongly correlated with patient outcomes in OSCC[51]. It could be used as an easy way for routine examination. However, some groups believed that the p16^{INK4a} expression alone didn't qualify as an efficient marker for HPV-positive OSCC and HNSCC [36,37,52,80,85,98]. Holzinger *et al*. concluded that the viral load and RNA pattern analysis are better prognostic markers than p16^{INK4a} alone in OSCC which is driven by HPV16 infection[37]. Schache *et al*. reported that a combination of p16^{INK4a} IHC and DNA qPCR showed 97% sensitivity and 94% specificity compared with the RNA qPCR [84]. Liang *et al*. also addressed this issue that neither HPV DNA nor p16^{INK4a} alone was associated with significant enhanced overall survival in OSCC [52]. Therefore, HPV-specific testing is still being investigated by using a single test or a combination of tests.

1.3.1 HPV-DNA detection

Up to now, HPV diagnostics has mainly been based on DNA detection including (1) non-amplified hybridization assays, such as southern transfer hybridization, dot blot hybridization and in situ hybridization. (2) Signal amplified hybridization assays, such as hybrid capture assays (HC2). (3) Target amplification assays, such as polymerase chain reaction (PCR) and in situ PCR [32].

HPV DNA has been detected in about 25% of HNSCC and 45%-100% cases were reported especially in OSCC [76]. Several studies have now shown that HPV16 accounts for 90% of HPV-positive OSCC. HPV18, the second most prevalent genotype, also had a significantly higher risk of developing OSCC [50]. It is therefore appropriate to test for HPV16 and HPV18 independently, which is termed HPV genotyping. Analysis of HPV DNA by PCR generic amplification and subsequent genotyping was performed in this study.

1.3.2 p16^{INK4a} immunostaining

p16^{INK4a} is a tumor suppressor protein that is encoded by three exons of the CDKN2a gene. It is a member of the INK4 class of cell-cycle inhibitors (INK4a), functions as an inhibitor of the cyclin-dependent kinases, decreasing pRb phosphorylation and preventing its dissociation from E2F transcription factor and the subsequent progression of the S phase of the cell cycle [93]. The disruption of p16^{INK4a} expression was associated with increased risk of a wide range of cancers [55]. p16^{INK4a} overexpression has been reported to be closely associated with HPV infection in OSCC and suggested to be a further indicator of active E7. This is because of E7-induced cell cycle activation and up-regulation of p16^{INK4a} through inactivation of the Rb pathway [42,50]. Therefore, p16^{INK4A} has been considered as a useful surrogate marker of carcinomas related to HPV infection. To detect p16^{INK4a} protein and its cellular localization, immunohistochemistry (IHC) has been established as a useful screening method.

1.4 Cancer stem-like cells (CSC)

1.4.1 Definition of putative CSC

The revolutionary concept that cancers are driven by cells with embryonic features can be traced back to the 19th century. It was first proposed by the German Nobel laureate and Charité pathologist Rudolf Virchow in 1855 that cancers may arise from the activation of dormant, embryonic cell remnants [73]. In 1990s, Lapidot *et al*. first discovered leukaemia-causing stem cells expressing the cell-surface markers CD34 and CD38. These cells were able to drive acute myeloid leukaemia in severe combined immune-deficient mice [47]. Until now, a growing body of research on various cancers strongly supports the hypothesis of CSC. CSC are a small subpopulation of cells which are distinguished from the bulk of the cells within the tumor that exhibit self-renewing capability and are believed responsible for tumor maintenance, growth and metastasis. CSC are less sensitive to chemotherapy and radiation and, when inoculated in immunocompromised mice, generate malignant cell populations that resemble the parental cancer in vivo [2,67]. The characteristics that define CSC are summarized in Table 1.5 [2]. As a result, it could possibly explain why many treatments seem to be effective initially but recurrence and metastasis occur later.

Table 1.5 Properties attributed to putative CSC [2].

- CSC initiate malignant tumors and drive neoplastic proliferation [56]
- CSC can recreate themselves by symmetric cell division [65]
- After transplantation to a suitable host, CSC recreate the heterogeneous phenotype of the originating tumor by asymmetric cell divisions [65]
- CSC are generally slow or non-dividing cells and thus relatively resistant to radiation and chemotherapeutic treatment [21]
- Compared to the "bulk"-tumor population, CSC express a distinct repertoire of biomarkers that can be used to define and isolate them [97]

1.4.2 Aldehyde dehydrogenases 1 (ALDH1) as a putative marker of CSC

To date, numerous studies have contributed to the identification and study of the CSC model in HNSCC/OSCC. CSC have been identified in head and neck cancer by appropriate markers like Oct4 [19], Nanog [19], CD44 [72], CD133 [103], the ATP-binding cassette transporter [31], and recently, high aldehyde dehydrogenase 1 (ALDH1) activity [15].

Human aldehyde dehydrogenases represent a multi-gene family of enzymes expressed at distinctive levels in multiple tissues and organs. To date, 17 isoforms of ALDH have been described. They are involved in the metabolism of aliphatic and aromatic aldehydes and critical for normal development and/or homeostasis, as each can be either relatively specific for the metabolism of a single endobiotic or primarily involved in the metabolism of potentially harmful xenobiotics [89].

ALDH1 is the prominent cytosolic ALDH isoform expressed in human cells, including normal and malignant epithelia, as well as hematopoietic stem cells. As a member of the ALDH enzyme family, ALDH1 catalyses the conversion of trans retinal to retinal acid, which are critical in regulating epithelial cell growth and differentiation that possibly contributes to the maintenance of an undifferentiated stem cell phenotype (Fig.1.7) [46,79,81].

It is evident now that ALDH1 is a more specific marker than any of the other phenotypes used in the past to identify the small population of highly tumorigenic cells present in HNSCC and other carcinomas as well [18,20,38,69]. Chen *et al*. showed that ALDH1^{+} cells from HNSCC were tumorigenic and displayed resistance towards radiotherapy [18]. In another study, the authors found that silencing of Bmi-1 significantly increased the sensitivity of HNSCC ALDH1^{+} cells to chemo-radiation and the degree of chemo-radiation-mediated apoptosis [17]. Therefore, ALDH1 expression holds out the promise of being a successful marker for therapeutic success and

prognosis. ALDH1 also correlates with cells undergoing epithelial-mesenchymal transition (EMT), a process that is thought to be an important requirement for metastasis [15].
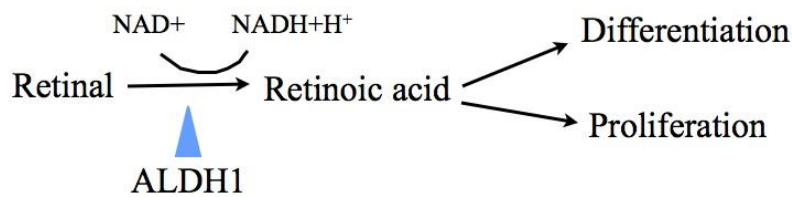
Figure 1.7 Oxidation of retinal to retinoic acid is catalyzed by ALDH1.

1.4.3 Role of CSC in the progression of the tumor

With the identification of CSC by appropriate markers, the development of in vitro studies, in vivo mouse models and the study of clinical patient samples, important advances have been achieved in the study of the role of CSC in the progression of malignancies. CSC may generate tumors through the stem cell processes of self-renewal and differentiation into multiple cell types. Further, the CSC state approached by carcinoma cells may undergo EMT, a process involved in metastasis dissemination [88].

EMT is a key step during embryogenesis enabling cells of epithelial phenotype to generate mesenchymal derivatives. Importantly, once the migrating mesenchymal cells have reached their destination, they can undergo a reverse EMT, a mesenchymal-epithelial transition (MET). Therefore, cells may revert back to the epithelial state from the mesenchymal phenotype. Although the EMT program is necessary for normal embryonic development, the aberrant activation of EMT contributes to various pathologic conditions, including fibrosis and carcinoma progression. Recent evidence suggests that cells undergoing EMT acquire stem cell-like properties, and EMT can also induce a CSC-like state in non-CSC [29,60,82]. It is assumed that the mesenchymal status is a condition to regain pluripotency. Normal stem cells and CSC may share a mesenchymal phenotype that enhances their ability to preserve stemness, to regain migratory properties, and to respond to different stimuli during expansion and differentiation. The yet unsolved question arises whether the metastatic cells disseminating from the primary tumor originate from resident stem cells in the tumor or if they derive from somatic tumor cells that have undergone EMT. The role of the EMT in enabling metastatic dissemination remains largely unclear. A recent hypothesis speculated that there are two subtypes of CSC within a

tumor. Intrinsic CSC, which exist in primary tumors from the very early stages of tumorigenesis, may be the oncogenic derivatives of normal-tissue stem or progenitor cells. Induced CSC occur as a consequence of the EMT. In this way, cancer cells can recruit a reactive stroma including fibroblasts, myofibroblasts, granulocytes, macrophages, mesenchymal stem cells, and lymphocytes. These reactive stromal cells release factors like Wnt, TGF-β, and fibroblast growth factor that may cause the neighboring cancer cells to undergo EMT and reach a CSC state (Fig. 1.8) [11].

Accumulating evidence revealed the importance of the role of EMT in metastatic dissemination with the CSC phenotype in HNSCC. We previously reported that ALDH1$^+$ putative CSC from HNSCC cell lines exhibited traits like self-renewal, quiescence, and increased expression of the stemness-related genes Oct3/4, Sox2, and Nanog. ALDH$^+$ putative CSC of HNSCC also possess higher invading capacity and upregulated EMT-markers, such as Snail1 and Twist, as well as a significantly increased expression of mesenchymal markers such as alpha-smooth muscle actin and Vimentin [15]. For HPV-related tonsillar cancer, it has been shown that downregulation of E-cadherin together with an upregulation of nuclear β-catenin, both characteristic for EMT, might be an early event in tumor progression [92]. It is also in line with the clinical observation of early lymphogenic metastasis in HPV-related OSCC. In oropharyngeal cancer cell lines, it has been shown that β-catenin nuclear accumulation and activation of Wnt signaling pathway are directly E6/E7 dependent [74]. Recently, Driessens *et al*. were the first to trace the CSC during the growth of tumor in a squamous skin tumor model by using a quantitative genetic labelling lineage with clonal analysis. By the observation of the clones of the labelled individual tumor cells at a range of time points, the papilloma was found to be sustained by a cellular hierarchy. This cellular hierarchy, which presented a minority population of tumor cells with stem-cell-like properties gives rise to a more transient progenitor cell pool. The stem-cell-like tumor cell division rate of twice per day was approximately four times faster than the progenitor cell division rate in the tumor. The authors also found that in invasive squamous carcinoma, the largest clones contained cells that contacted the stroma and endothelial cells as well as cells that had lost their intercellular cohesion with the rest of the clone, and presented with signs of EMT including a fibroblastic-like morphology. The size of the clone and proliferative potential showed a different pattern of behavior in contrast to the benign papilloma, consistent with geometric expansion of a single CSC population with limited potential for terminal differentiation [26]. Yang *et al*. found that RAC1 activation mediates Twist1-induced HNSCC cancer cell migration. These cells transited from non-motile, epithelial-like cells to motile mesenchymal cells which also were expressing a stem-like cancer cell phenotype [102].

In addition to the intrinsic regulation of CSC, a special environment, called tumor niche or microenvironment, may also play an interactive crosstalk role between them within the tumor. Krishnamurthy *et al.* observed that CSC were located in close proximity to blood vessels and that endothelial cell-initiated signalling can enhance the survival and self-renewal of head and neck CSC [45]. Campos *et al.* further revealed that endothelial derived factors inhibit anoikis of ALDH$^+$CD44$^+$ head and neck CSC [10].

Although there is accumulating experimental evidence for the role of the CSC model in the progression of the tumor, the clinical evidence for the CSC involvement in malignant progression is still sparse.
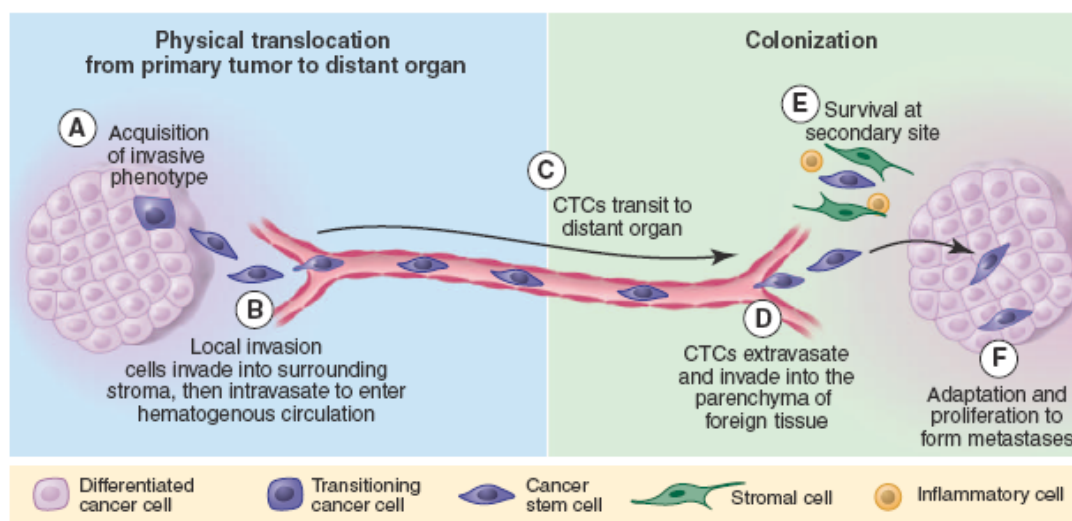
Figure 1.8 The metastatic cascade [11]. Metastasis can be envisioned as a process that occurs in two major phases: (1) physical translocation of cancer cells from the primary tumor to a distant organ and (2) colonization of the translocated cells within that organ. (A) To begin the metastatic cascade, cancer cells within the primary tumor acquire an invasive phenotype. (B) Cancer cells can then invade the surrounding matrix and blood vessels, where they are traveling through the circulation are circulating tumor cells (CTCs). They display properties of anchorage-independent survival. (D) At a distant organ, CTCs exit the circulation and invade the microenvironment of the foreign tissue. (E) At that foreign site, cancer cells must be able to evade the innate immune response and also survive as a single cell (or as a small cluster of cells). (F) To develop into an active macrometastatic deposit, the cancer cell must be able to adapt to the microenvironment and initiate proliferation.

1.4.4 Clinical relevance of CSC-targeted therapy

OSCC is divided into early-stage disease (Stage I/II), locally advanced disease (Stages III/IV) and recurrent/metastatic disease. Curative treatment is often but not always achieved in patients with early-stage disease through surgery or radiotherapy alone. Palliative chemotherapy, radio- or immunotherapy is applied in incurable disease. The majority of patients, more than two-thirds, with locally advanced disease receive a multi-modality-treatment involving surgery and adjuvant radio- and chemo- or immunotherapy. If surgery is not possible, it is substituted by primary radiotherapy. In patients with locally advanced tumors treated with surgery and/or chemo-radiotherapy loco-regional control can be gained but they will frequently develop a recurrence and/or metastasis. Widespread metastasis and radio- or chemo- resistance are the most common causes of long-term treatment failure. Thus, understanding the metastatic process of OSCC and the identification of factors predicting metastasis of OSCC are of high importance.

In a heterogenetic tumor, quiescent CSC form a very small proportion of the tumor, which may not be selected specifically as a target by drugs. In the initial stages of testing, the efficacy of cancer treatments is often measured by the ablated fraction of the maximal tumor mass, which comprise the bulk mass of the tumor containing differentiated or differentiating proliferating tumor cells in contrast to CSC (Fig 1.9). The presence of different tumor clones including CSC might be responsible for the therapy failure. Therefore, development of specific therapies targeted at CSC (Fig 1.9) holds out hope to decrease the intrinsic resistance to chemo- and radiotherapy and to improve survival and quality of life of patients.

Surgery
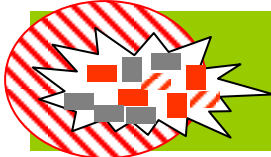
-potential to cure localized disease
-local side effects
-may be combined with other treatment modalities
-remaining CSC may recreate the tumor and metastases
-limited benefit for disseminated disease

Radiation/ chemotherapy

-potential to cure or control local and disseminated disease
-may be combined with surgery
-effect is dosage-dependent and may be limited by side effects
 or comorbidities and not sufficient for cure
-possibility of inherent radio-/chemo resistance
-response is determined by regression of "bulk"-tumor mass.
 CSC may remain to reconstitute the tumor.

CSC-directed therapy

-selective killing of CSC
-involution of bulk"-tumor due to limited self-renewal capacity
 without CSC
-systemic effect
-may be combined with other treatment modalities

 CSC   Heterogeneous tumor   Surgical margin

18

Figure 1.9 Illustration of therapeutic approaches for tumor elimination [2].

Conventional therapies of solid tumors aim unselectively at removing the bulk tumor mass by surgery with safe surgical margins depending on the tumor stage, often in combination with radiation and chemotherapy. Remaining CSC due to incomplete removal of the tumor or resistance to treatment may lead to tumor re-growth and ultimately failure of the therapy. Future CSC-targeted therapies could cut off the rejuvenating cell supply by CSC for the tumor and thereby lead to degeneration and involution of the tumor and lasting cure.

1.5 Objectives

Histopathological assessment of tissues from biopsy or surgical resection remains the cornerstone of cancer diagnosis and pathological staging in routine clinical practice. The TNM classification and staging system based on the size of the primary tumor, the presence of regional lymph node metastases, and distant metastases is one of the most important prognostic factors for OSCC. In addition, subtypes of OSCC with oncogenic HPV infections have been recognized. HPV infections are now considered as an important parameter of prognostic value for OSCC. Oral HPV infections need to be further studied and investigated so that it can guide us for individual treatment and future prevention programs, like HPV vaccination against oral HPV infections. Therefore, one aim of this study was to analyse the HPV-status in primary OSCC and its corresponding metastases, and to evaluate if there is a relationship between the histological grading, TNM classification and HPV infections.

The high mortality from OSCC is due to the development of distant metastases and the emergence of eventually inoperable local and regional recurrences that have low responsiveness to radio- or chemotherapy. Identification and characterization of CSC in OSCC yields new insights into the possible reasons for the metastasis/recurrence and poor prognosis. We designed this study in paired samples of primary OSCC and their respective lymph node metastases with the aim to evaluate the relevance of CSC-content between primary tumor and metastases, and in various stages of HPV-related and unrelated OSCC. Understanding the associations and relevance between HPV status and CSC content, in the progression of OSCC could support a rationale for the development of specific therapies for the distinct subgroups of HNSCC/OSCC and also for therapies targeting CSC directly.

2. Material and methods

2.1 Material

2.1.1 Equipment & Instruments

Equipment/Instrument	Producer
Captair filter	Erlab, Cologne, Germany
Centrifuge biofuge primo R	Heraeus, Hanau, Germany
Centrifuge megafuge 1.0	Heraeus, Hanau, Germany
Centrifuge minispin	Eppendorf AG, Hamburg, Germany
DISKUS version 4.80.3505-#412 software	HILGERS Technisches Büro, Königswinter, Germany
Freezer, −20 ℃	Bosch, Stuttgart, Germany
Freezer, −80 ℃	Thermo Scientific, Schwerte, Germany
Lab precision balance BL1500S	Sartorius AG, Goettingen, Germany
Lab water purification Systems Milli-Ro/Milli-Q Plus	Millipore Corporation, Billerica, MA, USA
LaminAir HB 2472 (Laminar flow workbench)	Heraeus Instruments, Hanau, Germany
Light microscope DMRXA	Leica, Heidelberg, Germany
Magnetic stirrer RET basic	IKA® Werke GmbH & Co.KG, Staufen, Germany
Memmert incubator model 200	Memmert GmbH + Co.KG, Schwabach, Germany
Microcentrifuge galaxy mini	VWR, Darmstadt, Germany
Microwave	Bosch, Stuttgart, Germany
Multipipettor	Eppendorf AG, Hamburg, Germany
Nikon ECLIPSE E200 microscope	Nikon Instruments, Düsseldorf,

	Germany
Olympus inverted microscope IMT-2	Olympus Optical Co., LTD., Hamburg, Germany
pH-Meter CG840	Schott-Geräter GmbH, Hofeim, Germany
Pipettes (10µl, 20µl, 100µl, 200µl, 1000µl)	Eppendorf AG, Hamburg, Germany
Pipetbody acu	Integra Bioscience GmbH, Fernwald, Germany
Refrigerator	Bosch, Stuttgart, Germany
Steam sterilizer, varioklav typ 300/400/500 EP-Z	Heraeus Instruments, Hanau, Germany
Vortex 2 genie	VWR, Darmstadt, Germany
Water bath TW12	Julabo, Seelbach, Germany
Weight BP-3105	Sartorius, Göttingen, Germany

2.1.2. Consumable supply

Consumable	Manufacturer
Cover glasses	Roth, Karlsruhe, Germany
Microtome blade stainless steel	Feather safety razor CO. LTD, Japan
Petri dishes	BD-Falcon, Heidelberg, Germany
Pipette tips (0.5-10 µl, 10-100 µl, 100-1000 µl)	Sarstedt, Nümbrecht, Germany
Pipette (2ml, 5ml, 10ml, 25ml)	BD-Falcon, Heidelberg, Germany
Reaction tube (0.5ml, 1ml, 2ml)	Sarstedt, Nümbrecht, Germany
SuperFrost® plus object slides	Superfrost Plus, Microm, Walldorf, Germany
Tube (15ml, 50ml)	BD-Falcon, Heidelberg,

Germany

2.1.3 Chemicals and Liquids

Chemical/Liquid	Manufacturer
Citric acid monohydrate	Merck, Darmstadt, Germany
Dimethyl sulfoxide (DMSO)	Sigma-Aldrich, Taufkirchen, Germany
Eosin	Roth, Karlsruhe, Germany
Ethanol 100 Vol. -% (MEK)	Merck, Darmstadt, Germany
Ethanol 96 Vol. -% (MEK)	Merck, Darmstadt, Germany
Ethanol 70 Vol. -% (MEK)	Merck, Darmstadt, Germany
Hydrochloric acid (HCl)	Roth, Karlsruhe, Germany
Mayer's Haematoxylin	DAKO, Glostrup, Denmark
Paraformaldehyde	Sigma-Aldrich, Taufkirchen, Germany
PBS	PAA, Cölbe, Germany
Sodium chloride (NaCl)	Merck, Darmstadt, Germany
Sodium hydroxide (NaOH)	Merck, Darmstadt, Germany
Tris(hydroxymethyl)-aminomethane (Tris-base)	Merck, Darmstadt, Germany
Tris(hydroxymethyl)-aminomethane-hydrochlorid (Tris-HCl)	Merck, Darmstadt, Germany
Tri-sodium citrate dihydrate	Merck, Darmstadt, Germany
Triton X-100	Sigma-Aldrich, Taufkirchen, Germany
Tween 20	Roth, Karlsruhe, Germany
Trypan blue	Sigma-Aldrich, Taufkirchen, Germany
Eukitt® quick-hardening mounting medium	Sigma-Aldrich, Steinheim, Germany
Xylene	J.T. Baker, Griesheim, Germany

2.1.4 Antibodies

Antibody	Manufacturer
Mouse anti-human p16^{INK4a} (monoclonal,clone DCS-50)	NeoMarkers, Fremont, CA, USA
Mouse anti-human ALDH1A1 (monoclonal, Clone 44)	BD Biosciences, San Jose, CA, USA

2.1.5 Commercial Solutions and Kits

Solution/Kit	Manufacturer
Antibody diluent solution	DAKO, Glostrup, Denmark
Normal goat serum	Invitrogen, Frederick, MD, USA
Peroxidase-blocking solution	DAKO, Glostrup, Denmark
Mouse primary antibody isotype control	DAKO, Glostrup, Denmark
Target retrieval solution pH 9.0	DAKO, Glostrup, Denmark
Target retrieval solution pH 6.0	DAKO, Glostrup, Denmark
Envision system-HRP Mouse	DAKO, Carpinteria, CA, USA
QIAamp Mini tissue kit	Qiagen, Hilden, Germany
Platinum Taq DNA polymerase	Life Technologies, Darmstadt, Germany
QIAquick PCR purification kit	Qiagen, Hilden, Germany
ZeroBlunt-Topo-PCR-Cloning Kit	Invitrogen, Leek, Netherlands

2.1.6 Solutions and Buffers

10×TBS (pH7.4)	**1000 ml**
Tris-base	9 g
Tris-HCl	68.5 g
NaCl	87.8 g
ddH$_2$O	up to 1000 ml

Adjusting the pH to 7.4.

Stored at room temperature (RT).

10×TBST(pH7.4, 0.05% Tween20)	**1000 ml**
10×TBS (pH7.4)	1000 ml
Tween 20	5 ml

Stored at RT.

10×Citrate buffer (pH6.0)	**1000 ml**
Citric acid	3.78 g
Trisodiumcitrate dihydrate	24.21 g
ddH$_2$O	up to 1000 ml

Adjust the pH to 6.0

Stored at RT or 4℃ for longer storage.

10×Tris-EDTA buffer (pH9.0, 0.05%Tween 20)	**1000 ml**
Tris	12.1 g
EDTA	3.7 g
ddH$_2$O	up to 1000 ml

Adjusting the pH to 9.0 if necessary.

Tween 20	5 ml

Stored at RT or 4 ℃ for longer storage.

2.1.7 Tissue samples

This study was approved by the internal review board of the University of Cologne, Germany and provided to us through a collaboration. Only patients who had no history of previous malignancies were included. Tumor specimens and normal mucosa from sites distant from the tumor (at least 2 cm) were obtained during surgery or diagnostic panendoscopy. One part of them was stored at −80 °C until further processing. The remaining part of each tumor was processed for routine histopathology. Data on the histological stage of tumor, differentiation and the TNM classification were retrieved from the pathology database and patient charts. 40 paired samples of primary OSCC and corresponding lymph node metastases were selected on the basis of availability of sufficient fresh-frozen tumor tissue with 70% tumor cells and high quality and sufficient tumor DNA.

2.2 Methods

2.2.1 DNA isolation

Tumor tissues were processed with the QIAamp Mini Tissue Kit (Qiagen GmbH, Hilden, Germany) for DNA isolation according to the manufacturer's protocol. The main QIAamp DNA purification procedure comprises 4 steps as follows: 25 mg tumor tissues were grinded and lysed with proteinase K at 56 ℃ overnight, the entire lysate was transferred to the QIAamp MinElute column, washed with provided buffers, finally 20–100 µl buffer was applied to elute the DNA from the membrane of QIAamp MinElute column.

2.2.2 Polymerase chain reaction (PCR) for HPV sequencing and typing

Human papillomavirus sequences were detected by highly sensitive nested PCR protocols with degenerate primers A10/A5-A6/A8. 10 µl of purified total cellular DNA was employed in each PCR reaction. Negative controls (water or human placental DNA) instead of patient samples were included in each PCR run.

Primers A5 and A10 (5'-TATTYTSCTWCTCCYAGTGG-3' and 5'-CKTCCCAARGGAWAYTGRTC-3'; HPV16 nt 6507-6526 and 7033-7014) were used for first-step PCR, and A6 and A8 (5'-GCM-CAGGGMCAYAAYAATGG-3' and 5'-CAAARTTCCARTCYTC- CAA-3'; HPV16 nt 6582-6601 and 6849-6831) for second-step PCR.

The reactions were run in a total volume of 50 μL, containing 50 mM KCl, 10 mM Tris-HCl pH 8.8, 3.6 mM (first-step PCR) or 1.5 mM (second-step PCR) MgCl2, 0.05% (wt/vol) gelatine, 200 mM of each dNTP, 1 mM of primers, and 2.6 U of Expand High Fidelity PCR System (Boehringer, Mannheim, Germany). The procedure (T3 Thermocycler, Biometra, Goettingen, Germany) included: 180 s at 95 ℃, followed by five cycles of 45 s/95 ℃, 45 s/50 ℃, and 90 s/72 ℃, followed by 30 cycles of 45 s/95 ℃, 45 s/56 ℃, and 90 s/72 ℃ (first-step PCR) and 180 s at 95 ℃, followed by 35 cycles of 45 s/95 ℃, 45 s/56 ℃, and 90 s/72 ℃ (second-step PCR). 3 μL of the first-step PCR reaction served as the template for second-step PCR. Human papillomavirus typing was performed by sequencing of PCR products and comparison of the obtained sequences with an HPV database. Direct sequence analysis of purified PCR products (QIAquick PCR purification kit, Qiagen, Hilden, Germany) was carried out with an ABI Prism 377 DNA sequencer using the Taq FS BigDye-Terminator cycle sequencing method (PE Applied Biosystems, Weiterstadt, Germany). Additionally, A6/A8 PCR products (270 base pairs) were cloned into the vector pCR-Blunt II-Topo using the ZeroBlunt-Topo-PCR-Cloning Kit (Invitrogen, Leek, Netherlands). Clones that carried an EcoRI insert of the expected size were sequenced as mentioned above. For HPV typing, the sequence information obtained was compared with an HPV database.

2.2.3 Sequence analysis

Sequence analysis was performed using the BLAST 2.0 and MacVector 7.0 (Oxford Molecular Group PLC, U.K.) program packages. GenBank, EMBL, DDJB, and PDB served as sequence databases.

2.2.4 Hematoxylin eosin (HE) staining

HE staining was performed for histological investigation of sections to determine the tumor content. Tissue specimens were fixed in 4% buffered formaldehyde and embedded in paraffin. Consecutive 4 μm thick sections were cut from tissue blocks and mounted on glass slides (Superfrost Plus, Microm, Walldorf, Germany). Sections were dried at 60 ℃ for 2 hours. This was followed by de-paraffinisation in xylene 2×5 min, and rehydration in a series of decreasing ethanol concentrations, ending in distilled water. Sections were incubated in hematoxylin for 5-10 minutes, followed by three washing steps in tap water for 3 minutes each. Next, sections were

bathed in 0.1% eosin (in ddH2O), followed by washing in ddH2O for 2 minutes. Sections were dehydrated by an ascending ethanol series. After two rounds of xylene (2 minutes each), sections were mounted and dried overnight.

2.2.5 Immunohistochemistry (IHC)

Sections were prepared as mentioned above. Immunohistochemical staining was performed using the two-step IHC detection reagent following the manufacturerś instruction (Envision system-HRP Mouse, DAKO, Hamburg, Germany). After microwave treatment (twice for 7 min at 600 W in 10 mM citrate buffer, pH 6.0) for antigen retrieval, sections were cooled to room temperature. Endogenous peroxidase activity was blocked by immersing slides in Chem Mate Peroxidase-Blocking Solution (DAKO) 10 min at room temperature. Slides were incubated with mouse monoclonal antibody specific for p16^{INK4a} (1:100 dilution, clone DCS-50; NeoMarkers, Fremont, CA, USA) or mouse monoclonal antibody specific for ALDH1A1 (1:100 dilution, clone 44; BD Biosciences, San Jose, CA, USA) for 2 hours, followed by addition of HRP-labeled rabbit anti-mouse secondary antibody. Between each step, sections were rinsed twice in TBS 3×5 min. Immunoreactive proteins were visualized with 3,3-diaminobenzidine for 10 min, raised in distilled water, and counterstained with Mayer's haematoxylin. Then the sections were dehydrated in increasing concentrations of ethanol, finishing with xylene 2×5 min. Sections were mounted, and analyzed using a standard microscope. Positive and negative controls were included in each run for quality control of the immunoreactivity. Tissues from previous tonsil squamous cell carcinoma with high p16^{INK4a} or ALDH1 expression served as positive controls . A mouse isotype control (DAKO) was used to replace the primary antibody as negative controls.

2.2.6 Evaluation of staining

Three independent experienced observers, blinded to the patients' clinical information, performed semiquantitative evaluation of the slides. Discrepancies were resolved by a consensus meeting using a multiheaded microscope. Areas of carcinoma tissue within the samples and the p16 and ALDH1 expression pattern were evaluated by comparing the intensity and cellular localization of immunoreactivity with positive and negative controls. Usually more than 1000 cells in five randomly selected fields of tumor tissue were analyzed for each section at a magnification of x400 to determine percentage labeling indices. p16^{INK4a} expression was scored

as positive if there was strong and diffuse nuclear and cytoplasmic staining in more than 60% of the tumor[41,77]. For ALDH1, all cases were classified as negative (no positive tumor cells) and positive. Moreover, the immunoreactivity of ALDH1 was graded into four categories to enable statistical analysis: grade 0: 0-5% positive cells; grade 1: 5–25%; grade 2: 26–50% and grade 3: >50%. In tumors showing heterogeneous expression, the grade was judged according to the predominant pattern.

2.2.7 Statistical analysis

Statistical analysis was performed using the STATA 9.0-software (StataCorp LP, TX, USA). Categorical variables were described by percentages and frequencies, and numerical variables were represented as mean $\pm$ SD. Qualitative data were compared using the chi-square or Fisher exact test, as appropriate. For continuous data, between-group comparisons were performed by either the Mann-Whitney or the Student t test, depending on the normality of each variable. All statistical comparisons were 2-sided. A p-value of <0.05 was regarded as statistically significant.

3 Results

3.1 Characteristics of patients

Of the 40 OSCC tumors, the patient ages ranged from 38 to 79 years (median 57.8 years). 79% patients were males and 27.5% were females. In 17.5% the OSCC was located in the tongue and in 82.5% in the tonsil. The pathological tumor stage according to the TNM classification was as follows: pT1: 11 (27.5%); pT2: 21 (52.5%); pT3: 8 (20%); pN1: 15 (37.5%); pN2+pN3: 25 (62.5%). As tonsil tumors tend to be non-keratinizing or basaloid, grading is sometimes ambiguous. Therefore, 6 cases (22%) were classified as grade 1-2 or 2-3 (Table 3.1).

Table 3.1 Characteristics of patients

Parameter	n (%)
Sex	
Female	11 (27.5)
Male	29 (72.5)
Site	
Tongue	7 (17.5)
Tonsil	33 (82.5)
Tumor Stage	
pT1	11 (27.5)
pT2	21 (52.5)
pT3	8 (20)
Nodal status	
pN1	15 (37.5)
pN2+pN3	25 (62.5)
Histology	
G1	1 (2.5)
G1-2, G2	19 (47.5)
G2-3, G3	20 (50)

3.2 HR-HPV DNA detection results

20 (50%) primary tumors were HPV-DNA positive. Eight of 20 HR-HPV-DNA-positive primary tumors had metastases where no HPV-DNA was detectable. All 20 HPV-DNA-negative primary tumors had negative HPV-specific PCR findings for their metastases (Table 3.2).

3.3 Tumor tissue determined by HE staining

Tumor tissues were identified and determined by HE staining. Nuclei were stained with hematoxylin which presented by blue color. After being counterstained with eosin, the cytoplasm was presented in pink color (Figure 3.1). 40 pairs of patients' samples were identified with tumor content.
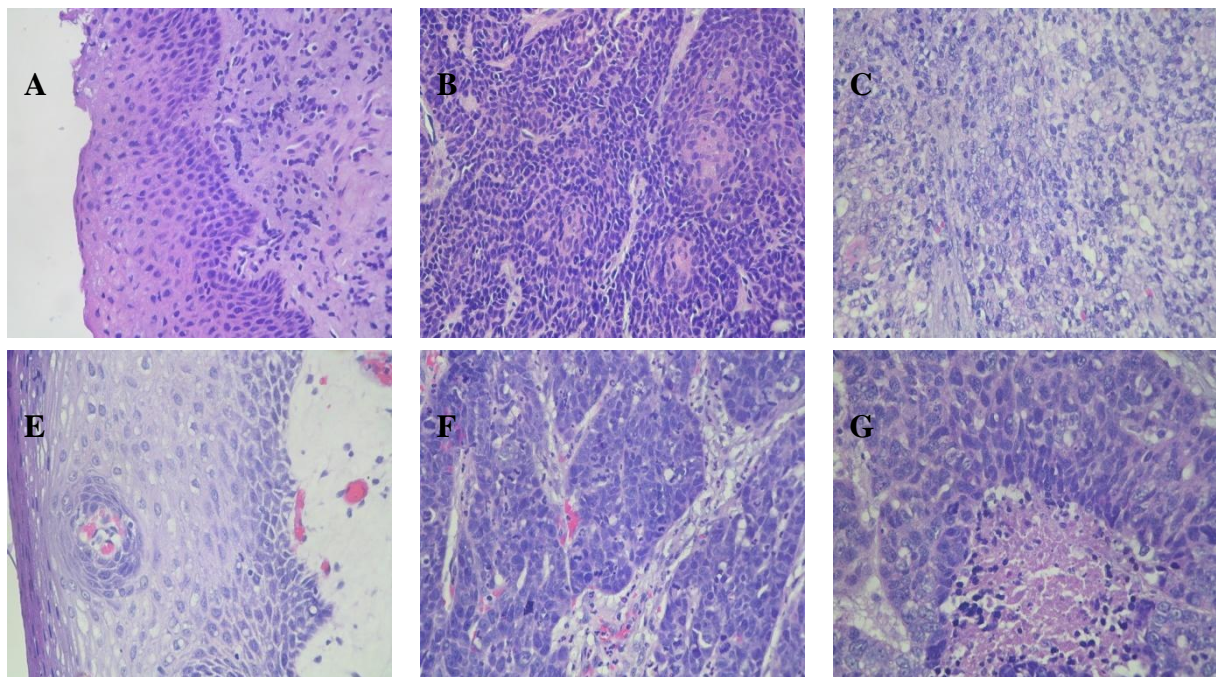
Figure 3.1 HE stainings in OSCC. (A) Normal epithelium of tongue. (B) Tongue cancer. (C) Corresponding metastases of tongue cancer. (D) Normal epithelium of tonsil. (E) Tonsillar cancer. (F) Corresponding metastases of tonsillar cancer. (400X magnification)

3.4 Light microscopic quantification of p16^{INK4a} staining

p16^{INK4a} could be detected in primary tumors and in metastases. Localization of p16^{INK4a} was found to be nuclear and cytoplasmic. Figure 3.2 shows examples of the IHC staining of p16^{INK4a} in OSCC.

All 23 p16^{INK4a}-negative primary tumors had p16^{INK4a}-negative metastases. In 4 out of 17 p16^{INK4a}-positive primary tumors the corresponding metastasis was p16^{INK4a}-negative.
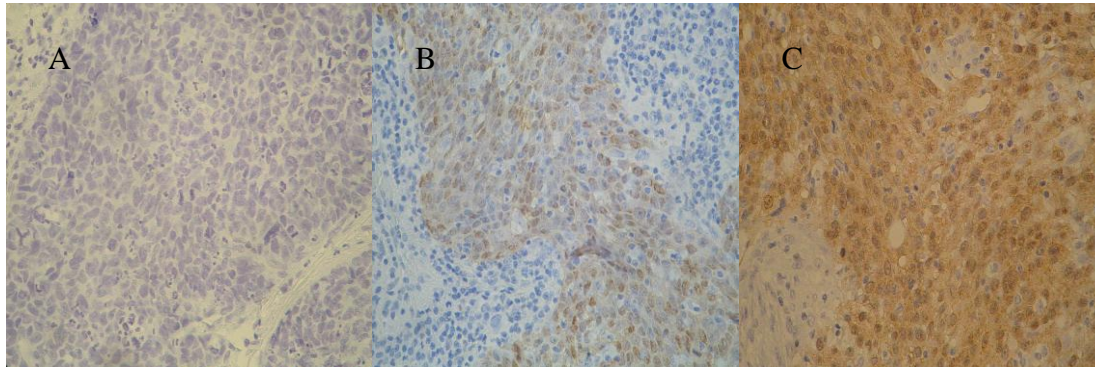
Figure 3.2 p16^{INK4a} positivity in OSCC. (A) Negative expression in primary tumor. (B) Positive expression in primary tumor. (C) Positive expression in corresponding metastases. (400X magnification).

3.5 Correlation between HR-HPV status, p16^{INK4a} expression and clinico-pathological parameters

The correlation between positive HR-HPV status and p16^{INK4a} expression in total specimens (p<0.001), primary tumors (p<0.001), and metastases was highly significant (p<0.001) (Table 3.2). 80% of HR-HPV-DNA-positive primary tumors co-expressed p16^{INK4a} and 95% of HPV-DNA-negative tumors were p16^{INK4a}-negative. 92% of HR-HPV-DNA-positive metastases were p16^{INK4a}-positive and 93% of HPV-DNA-negative metastases were p16^{INK4a}-negative. Positive p16^{INK4a}-status has a specificity of 90% for HR-HPV-DNA positivity in this study. No significant association was observed between HPV-DNA status or p16^{INK4a} expression and clinico-pathological parameters.

Table 3.2 HPV-DNA detection and expression of p16^{INK4a} and ALDH1 in primary tumors and metastases.

	HPV-DNA detection			p16^{INK4a} expression			ALDH1 expression		
	Neg, no (%)	Pos, no (%)	P-value	Neg, no (%)	Pos, no (%)	P-value	Neg, no (%)	Pos, no (%)	P-value
Total (n=80)	n=48	n=32		n=50	n=30		n=9	n=71	
Origin									
Primary (n=40)	20(50)	20(50)	0.068	23(58)	17(42)	0.356	5(13)	35(87)	0.723
Metastasis (n=40)	28(70)	12(30)		27(68)	13(32)		4(10)	36(90)	
HPV-DNA detection									
HPV$^+$ (n=32)				5(16)	27(84)	<0.001	3(9)	29(91)	0.665
HPV$^-$ (n=48)				45(94)	3(6)		6(12)	42(88)	
p16^{INK4a} expression									
p16^{INK4a+} (n=30)							2(7)	28(93)	0.315
p16^{INK4a-} (n=50)							7(14)	43(86)	
Primary (n=40)	n=20	n=20		n=23	n=17		n=5	n=35	
Age (years)	55.7±9.49	59.95±10.46	0.1863	56.48±9.05	59.65±11.37	0.333	58.4±5.08	57.74±10.66	0.894
Sex									
Female (n=11)	6(55)	5(45)	1.000	7(64)	4(36)	0.726	2(18)	9(82)	0.603
Male (n=29)	14(48)	15(52)		16(53)	13(47)		3(10)	26(90)	
Primary Site									
Tongue (n=7)	5(71)	2(29)	0.407	4(57)	3(43)	1.000	0	7(100)	0.565
Tonsil (n=33)	15(45)	18(55)		19(58)	14(42)		5(15)	28(85)	
Tumor Grade									
G1 (n=1)	0	1(100)	0.591	0	1(100)	0.438	1(100)	0	0.009
G1-2, G2 (n=19)	10(53)	9(47)		12(63)	7(37)		2(11)	17(89)	
G2-3, G3 (n=20)	10(50)	10(50)		11(55)	9(45)		2(7)	28(93)	
Tumor Stage									
pT1 (n=11)	4(36)	7(64)	0.505	5(45)	6(55)	0.637	2(18)	9(82)	0.270
pT2 (n=21)	11(52)	10(48)		13(62)	8(38)		1(5)	20(95)	
pT3 (n=8)	5(63)	3(37)		5(63)	3(37)		2(25)	6(75)	
HPV-DNA detection									
HPV$^+$ (n=20)				4(20)	16(80)	<0.001	3(15)	17(85)	1.000
HPV$^-$ (n=20)				19(95)	1(5)		2(10)	18(90)	
p16^{INK4a} expression									
p16^{INK4a+} (n=17)							2(12)	15(88)	1.000
p16^{INK4a-} (n=23)							3(13)	20(87)	
Metastasis (n=40)	n=28	n=12		n=27	n=13		n=4	n=36	
N-Stage									
pN1(n=15)	12(80)	3(20)	0.477	11(73)	4(27)	0.730	4(27)	11(73)	0.015

pN2, pN3(n=25)	16(64)	9(36)	16(64)	9(36)		0	25(100)	
HPV-DNA detection								
HPV$^+$ (n=12)			1(8)	11(92)	<0.001	0	12(100)	0.297
HPV$^-$ (n=28)			26(93)	2(7)		4(14)	24(86)	
p16^{INK4a} expression								
$^{p16INK4a+}$ (n=13)						0	13(100)	0.284
$^{p16INK4a-}$ (n=27)						4(15)	23(85)	

Abbreviation: Neg, negative; Pos, positive; n, no, number.

3.6 Light microscopic quantification of ALDH1 staining

ALDH1 could be detected in primary tumors and in metastases. ALDH1 positivity was found in the cytoplasm of tumor cells. ALDH1 expression in poorly differentiated, moderately differentiated and well-differentiated OSCC is illustrated in figure 3.3.
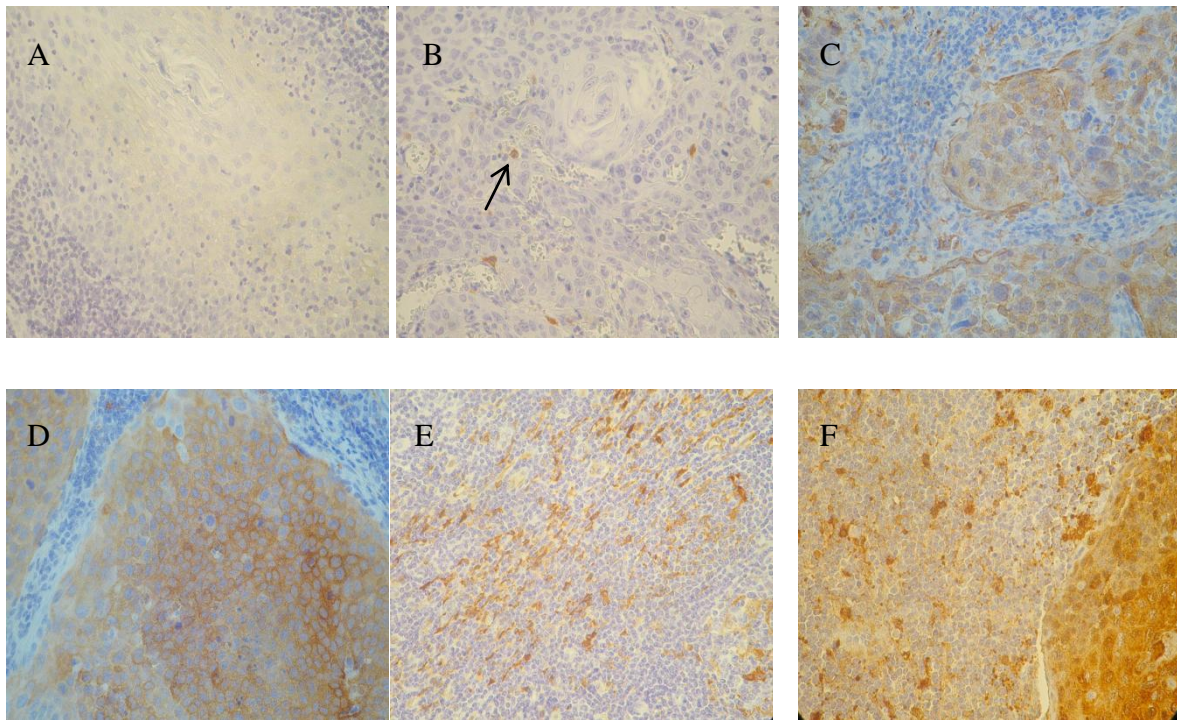
Figure 3.3 Immunohistochemical identification of ALDH1^{+} tumor cells. (A) Negative expression in OSCC. (B) Positive expression in well-differentiated OSCC (HPV[+]). (C) Positive expression in moderately differentiated OSCC (HPV[-]). (D) Positive expression in mediated differentiated OSCC (HPV[+]). (E) Positive expression in poorly differentiated OSCC (HPV[-]). (F) Positive expression in metastases (HPV[-]). (400x magnification)

3.7 Grading of ALDH1 staining

The immunoreactivity of ALDH1 positively stained cells was graded into four categories presented in figure 3.4.
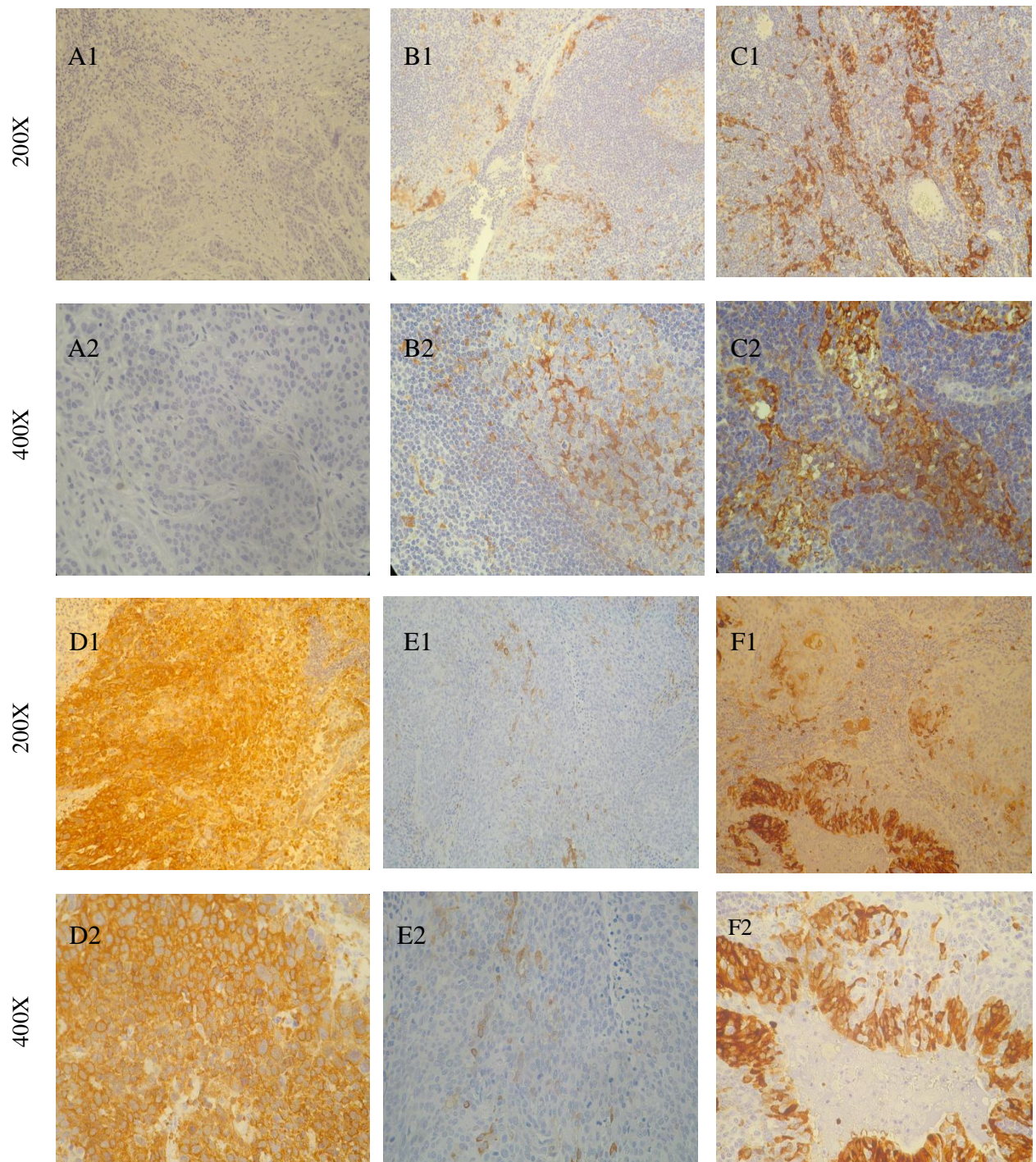
Figure 3.4 Representative examples of ALDH1-specific immunohistochemical staining in oropharyngeal squamous cell carcinoma (OSCC) (A1-2) with grade 0; (B1-2) with grade 1; (C1-2) with grade 2; (D1-2) with grade 3. (E1-2) Distribution of ALDH1 expression in primary tumor tissue. (F1-2) Representative ALDH1 expression in corresponding metastasis.

3.8 Distribution of ALDH1 positive cells in non-tumor sites

Except tumor area, ALDH1$^+$ tumor cells were also observed in adjacent normal epithelial as shown in figure 3.5. A. And in some cases, ALDH1$^+$ stroma cells were found near the vessels. Minor salivary glands were also positively stained with ALDH1 in some cases.
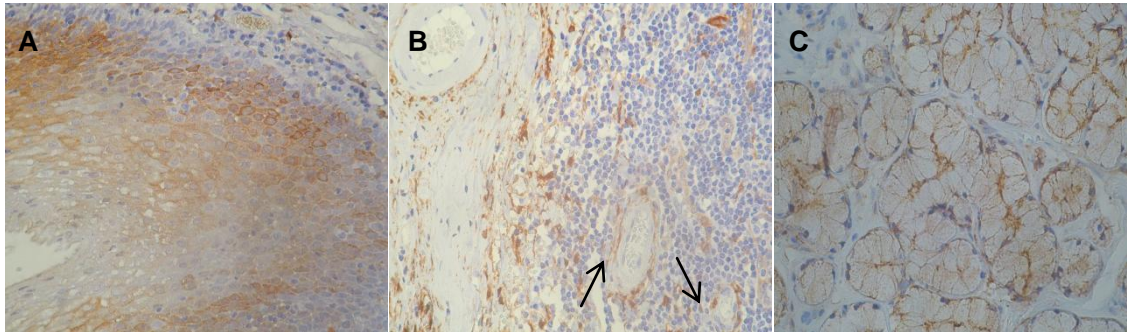
Figure 3.5 Immunohistochemical staining of ALDH1$^+$ cells in non-tumor sites. (A) Normal epithelium with ALDH1 positive staining. (B) Proliferating vessels (black arrows) with ALDH1+ cells in their vicinity. (C) ALDH1$^+$ cells can be seen in minor salivary glands. (400x magnification)

3.9 ALDH1 expression and its correlation with clinico-pathological parameters

Expression of ALDH1 was detected in 87.5% primary tumors and in 90% of the metastases. ALDH1 positivity was significantly correlated with lower tumor differentiation (p=0.009) and higher pN classification (p=0.015) (Table 3.2).

Subsequently, samples were divided into groups with different ALDH1 expression grades (0-3) (Figure 3.6). Higher expression grades of ALDH1 were also more frequent in primary tumors with lower tumor differentiation (p=0.022) and higher pN classification, (p= 0.025) (Table 3.3). Next, we analyzed the HPV-status, p16^{INK4a}, and ALDH1 positivity in metastases, however no significant correlation was found. In contrast, ALDH1 expression grades were significantly elevated in metastases versus primary tumors (p=0.012) (Table 3.3) regardless of the ALDH1 grades of the corresponding primary tumors.

3.10 Correlation between HR-HPV DNA status, p16^{INK4a} and ALDH1 expression

Comparing HPV negative and positive tumors, there was no correlation between ALDH1 expression and HPV status in total specimens (p=0.665), primary tumors (p=1) and metastases (p=0.297) (Table 3.2). Significant correlations, however, were found between higher ALDH1 expression grades and negative HPV status for primary tumors (p=0.004), but not for metastases

(p=0.429) (Table 3.3). There was no correlation between ALDH1 expression and p16^{INK4a} expression for primary tumors (p=1) and metastases (p=0.284) (Table 3.2). There was also no significant correlation between ALDH1 expression grade and p16^{INK4a} expression between primary tumors (p=0.2) and metastases (p=0.362) (Table 3.3).

Finally, subgroups of HR-HPV-DNA$^+$/p16^{INK4a+} and HPV-DNA$^-$/p16^{INK4a-} tumors were correlated with ALDH1 expression. There were no correlations between these two groups concerning ALDH1 positive and negative expression in primary tumors or metastases. But as expected from the above results, when comparing these subgroups concerning ALDH1 expression grades, we found that HPV-DNA$^+$/p16^{INK4a+} primary tumors exhibit significantly lower ALDH1 expression grades whereas HPV-DNA$^-$/p16^{INK4a-} primary tumors presented with higher ALDH1 grades (p=0.038) (Fig 3.6, Table 3.4). There were no similar findings for metastases (p=0.441) (Fig 3.6, Table 3.4).
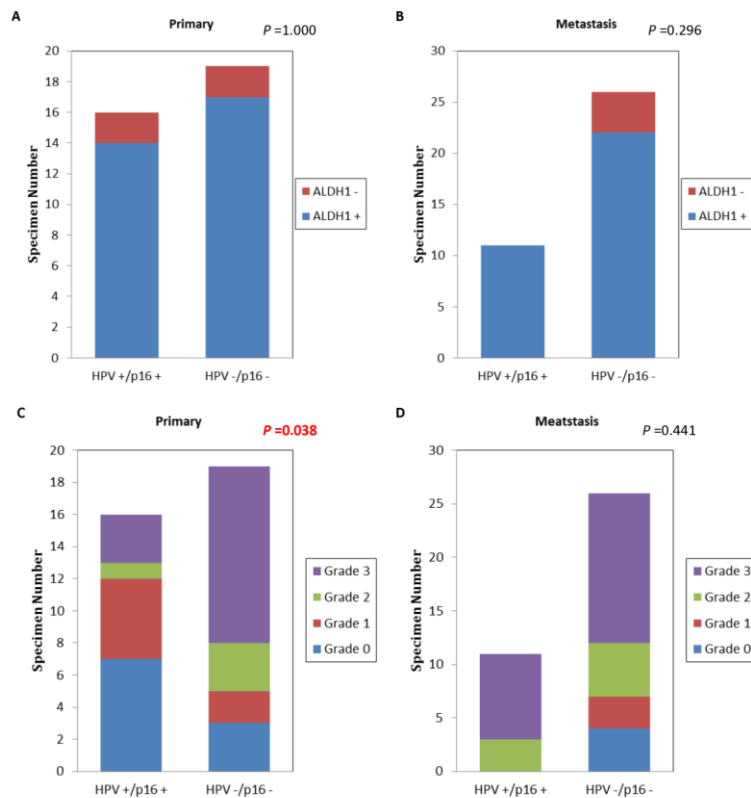
Figure 3.6 Correlation between HPV-DNA detection with p16^{INK4a} expression and ALDH1 expression. Distribution of ALDH1 positivity between HR-HPV-related (HPV$^+$/$^{p16INK4a+}$) and HPV-unrelated (HPV$^-$/p16^{INK4a-}) tumors in primary OSCC (A) or nodal metastases (B). Distribution of the percentage of ALDH1 tissue expression expressed as grade 0-3 compared between HR-HPV-related (HPV$^+$/p16^{INK4a+}) and HPV-unrelated (HPV$^-$/p16^{INK4a-}) tumors in primary OSCC (C) or nodal metastases (D).

Table 3.3 Correlation between ALDH1 grade and clinico-pathological characteristics.

Characteristic	n	ALDH1 expression grade				p-value
		0	1	2	3	
		number (%)				
Primary site						
Tongue	7	2(29)	2(29)	2(29)	1(14)	0.725
Tonsil	33	12(36)	5(15)	3(9)	13(39)	
Origin						
Primary	40	14(35)	7(17)	4(10)	15(38)	0.012
Metastases	40	4(19)	3(8)	8(20)	25(62)	
Tumor differentiation grade						
G1	1	1(100)	0	0	0	0.022
G1-2, G2	19	8(42)	6(32)	2(10)	3(16)	
G2-3, G3	20	5(25)	1(5)	2(10)	12(60)	
Tumor (T) Stage						
pT1	11	6(55)	3(27)	0	2(18)	0.206
pT2	21	5(24)	4(19)	2(10)	10(48)	
pT3	8	3(38)	0	2(25)	3(38)	
Nodal (N) Stage						
pN1	15	4(27)	1(7)	1(7)	9(60)	0.025
pN2, pN3	25	0	2(8)	7(28)	16(64)	
HPV-DNA in total specimens						
HPV$^+$	32	11(34)	5(16)	4(13)	12(38)	0.130
HPV$^-$	48	7(15)	5(10)	8(17)	28(58)	
HPV-DNA in primaries						
HPV$^+$	20	11(55)	5(25)	1(5)	3(15)	0.004
HPV$^-$	20	3(15)	2(10)	3(15)	12(60)	
HPV-DNA in metastases						
HPV$^+$	12	0	0	3(25)	9(75)	0.429
HPV$^-$	28	4(14)	3(11)	5(18)	16(57)	
p16^{INK4a} expression in total specimens						
p16^{INK4a+}	30	7(23)	5(17)	4(13)	14(47)	0.831
p16^{INK4a-}	50	11(22)	5(10)	8(16)	26(52)	
p16^{INK4a} expression in primaries						
p16^{INK4a+}	17	7(41)	5(29)	1(6)	4(24)	0.200
p16^{INK4a-}	23	7(30)	2(9)	3(13)	11(48)	
p16^{INK4a} expression in metastases						
p16^{INK4a+}	13	0	0	3(23)	10(77)	0.362
p16^{INK4a-}	27	4(15)	3(11)	5(19)	15(56)	

Table 3.4 Correlation between HPV-DNA detection with p16^{INK4a} expression and ALDH1 expression.

| Characteristic | n | ALDH1$^+$ | ALDH1$^-$ | p-value | ALDH1 expression grade | | | | p-value |
| | | | | | 0 | 1 | 2 | 3 | |
					number (%)				
Primary tumor									
HR-HPV$^+$/p16^{INK4a+}	16	14(88)	2(12)	1.000	7(44)	5(31)	1(6)	3(19)	0.038
HR-HPV$^-$/p16^{INK4a-}	19	17(89)	2(11)		6(32)	2(11)	3(16)	11(58)	
Metastases									
HR-HPV$^+$/p16$^{INK4a +}$	11	11(100)	0	0.296	0	0	3(27)	8(73)	0.441
HR-HPV$^-$/p16^{INK4a-}	26	22(85)	4(15)		4(15)	3(11)	5(19)	14(54)	

4 Discussion

In elucidating OSCC tumorigenesis, CSC research is currently a promising field that could lead to a better understanding of the formation of recurrence, metastasis, and resistance to radio- and chemotherapy. In the current study, we specifically focused on: (1) HPV infection with the clinical and histopathological characteristics of OSCC, (2) The clinical and histopathological characteristics of OSCC and its corresponding metastases in relation to ALDH1 positive CSC, (3) CSC frequency in relation to HPV infection.

4.1 Relevance of HPV infection in OSCC and its corresponding metastases

With regard to the etiology of OSCC, HPV infection was explored in the present study. Herein, in primary OSCC, 20 (50%) cases were HPV-DNA positive, and 17 (42.5%) cases were p16^{INK4a} positive. In metastases, 12 (30%) cases were HPV-DNA positive, and 13 (32.5%) cases were p16^{INK4a} positive. Robinson *et al.* reviewed 6 studies with 496 tumors in total. They found an HPV negative/p16^{INK4a} positive status in 5% and HPV positive/p16^{INK4a} negative status in 8% of the investigated cases [80]. We found a similar inconsistency in this study. 80% of HR-HPV-DNA positive primary tumors co-expressed p16^{INK4a} and 95% of HPV-DNA negative tumors were p16^{INK4a}-negative. 92% of HR-HPV-DNA positive metastases were p16^{INK4a}-positive and 93% of HPV-DNA negative metastases were p16^{INK4a}-negative. Possible explanations for these differences are the limitations of the detection methods or concomitant representing false-positive results.

The findings of some studies evaluating the correlation of OSCC histological grading and TNM stage in relation to HPV infection were contradictory. It was reported that HPV$^+$ tumors are less differentiated than HPV$^-$ ones and present more frequently with nodal metastases. But HR-HPV$^+$ OSCC patients showed better survival than those with HPV$^-$ OSCC [8,63]. Our data didn't show the correlation of HPV or p16^{INK4a} expression with histological grading and TNM stage. Fewer samples or the fact that parameters evaluated are also accompanied with additional concurrent risk factors might explain this result.

Our data demonstrated a presence of viral DNA in cervical lymph nodes. HPV-DNA was identified in cervical LNs in 8 out of 20 patients with HPV-DNA positive OSCC. Most studies confirm that metastatic LNs tend to be HPV positive. But previous reports on cervical cancer and head and neck cancer showed that HR-HPV detection in metastatic LNs ranged from 20% to 100% [12,22,34,49,64]. Sample selection, detection methods, and virologic analyzing techniques could have influenced the results. In this study, we used HPV-DNA detection to determine the

HPV status of the tumors. If this is a limitation of the study remains unclear. Of note, in our study, HPV infection in the corresponding metastases also didn't show any association with histological grading and TNM stage while other studies had shown a positive correlation [9]. To determine the true presence of HPV in LNs of OSCC, different methods should be compared. To elucidate the clinical relevance of this information, a larger study population including subgroups of patients with early or late metastasis would be of importance.

4.2 Evidence of ALDH1^{+} CSC in primary OSCC

A number of groups have identified and isolated CSC enabling the characterization of these cells in HNSCC. ALDH1 populations may indeed harbor a subpopulation encompassing CSC of the tumor including HNSCC. In one study, ALDH1^{+}cells derived from HNSCC were tumorigenic and displayed resistance towards radiotherapy [18]. In another study, the authors found that the silencing of Bmi-1, a transcriptional repressor essential for maintaining the self-renewal abilities of adult stem cells and CSC, significantly increased the sensitivity of ALDH1^{+} HNSCC cells to chemo-radiation and the degree of chemo-radiation-mediated apoptosis [17]. Therefore, measuring ALDH1 expression holds out promise as a marker for therapeutic success and prognosis. But the relevance of ALDH1+ CSC in solid tumors is still sparse.

We found high expression rates (87%) of ALDH1^{+} CSC in primary OSCC tissues. In ALDH1 positive OSCC, the percentage of ALDH1 expressing tumor cells ranges from scatted distributions with less than 1% to a wide distribution with more than 50%. ALDH1 expressing tumor cells were found in all histological types including well differentiated, moderately differentiated and poorly differentiated OSCC. These results supported the existence of CSC in OSCC. On the other hand, it could be a possible explanation for tumor heterogeneity. Cancer has long been considered to be an evolutionary issue. In this way, tumor heterogeneity is thought to arise from clonal evolution. The hypothesis of the CSC model has now been proposed to explain tumor heterogeneity in a different way. A hierarchical organization in which a tumor arises from and is maintained by a small population of CSC was postulated. A CSC model was also postulated for the clonal evolution model. CSC may be genetically unstable resulting in clonal evolution that generates several distinct CSC clones in a tumor [16]. The stemness phenotype of CSC can be identified by different markers like CD44^{+}CD24^{-}, CD133, the ATP-binding cassette transporter, ALDH1, whereas the overlaps between different CSC groups were also found [2,15,68,101].

In primary OSCC, we also demonstrated that ALDH1 expression rates were related to lower tumor grades. Higher ALDH1 grades are found significantly associated with a lower grade of tumor differentiation and a higher nodal classification. This indicates that the frequency of CSC is related to poorly differentiated OSCC and the occurrence of nodal metastasis. Additionally, the frequency of CSC seems to be connected to the progression of OSCC and most likely plays a role in this process. Supporting these findings, numerous recent studies of carcinomas of different origins also presented traits of high-grade malignancy that could be specifically traced to the presence of CSC, implying that CSC may be the critical drivers of tumor progression [13,70].

4.3 ALDH1^{+} CSC in primary OSCC and its corresponding metastases

CSC have been defined by their most central trait, the ability to seed new tumors and metastases [11]. In our previous study in HNSCC cell lines, the invasiveness of tumor cells was explored and correlated to the CSC phenotype [15]. CSC reside in close proximity to blood vessels and can give rise to tumor endothelium [99]. It was reported [10] that endothelial-derived factors inhibit anoikis of ALDH^{+}CD44^{+} head and neck cancer stem cells. EMT is regarded a necessary process that empowers CSC to disseminate from primary tumors and to seed metastases. In order to understand the role of ALDH1^{+} CSC in the progression of OSCC, we analyzed their frequency and distribution in primary tumors and their metastases. Only few previous studies have comparatively studied CSC in primary tumors with their associated metastases so far. It was reported that increased ALDH1 expression in patients with breast cancer lymph node metastases serves as a prognostic factor of poor clinical outcome [68].

In our study the ALDH1 positive staining rates in metastatic lymph nodes were similar to its corresponding primary OSCC tissues. In the total case collection, metastasis did not display a significantly increased number of ALDH1^{+} cells when compared to the primary tumor. However, when the percentage of ALDH1^{+} cells in the materials were classified into grades 0-3, significant differences between primary tumor and corresponding lymph node metastases became obvious. In general a higher grade of ALDH1 expression was more frequently found in metastases and also correlated to higher nodal metastasis status of the patient. The observation that the numbers of CSC were increased in metastases may reflect the fact that successful seeding of metastases requires a more motile cellular phenotype that is supported by the ability of CSC to undergo EMT. An open question is whether the increase of CSC numbers manifests transiently e.g. in the initiation period during the metastatic colonization and decreases later or displays a stable state.

Consistent with our findings, recently, Malanchi *et al.* found, from a breast cancer model, that the relative size of the CSC population increased during the early period of metastatic colonization in the secondary target organ, i.e. lung [59]. In our study, metastases presented significantly higher grades of ALDH1 expression than the corresponding primary tumor. This evidence could also be a clue for the active function of CSC in the process of metastasis formation.

We show for the first time a significant association between ALDH1$^+$ OSCC and their nodal metastases. Taken together, the results of our former study of EMT capacity and ALDH association of HNSCC cell lines and the current data from clinical paraffin-embedded specimen show that ALDH1$^+$ CSC are highly invasive and may have metastatic ability. Recently, Xu *et al.* investigated the ALDH1$^+$ CSC-content of primary metastatic or non-metastatic HNSCC. ALDH1 expression in primary tumors correlated with lymph node metastasis. Patients with low ALDH1 expression levels in primary tumors had a better 5-year survival rate than those with high ALDH1 expression level [101].

4.4 ALDH1$^+$ CSC frequency in relation to HPV infection

We observed that lower ALDH1 grades in the primary tumors were seen in HPV-DNA positive tumors and higher grades in HPV-DNA negative primaries. This might reflect different initiating processes for carcinogenesis in both subgroups. In contrast, in metastases this difference was not seen, probably because of further, more general processes driving progression overcome the importance of special initiating processes like in HPV-driven carcinogenesis. By subgroup analyses, we found that HR-HPV-DNA$^+$/p16^{INK4a+} primary tumors exhibited lower ALDH1 expression grades representing a lower number of CSC while HPV-DNA$^-$/p16^{INK4a-} primary tumors had higher ALDH1-grades representing a higher CSC frequency. Our data support an existence of distinct tumor cell characteristics defined by the HPV status. This difference is reflected by different ALDH1 grading in the primary tumors. On the other hand, HPV-related OSCC develop early lymphogenic metastasis. This might be due to HPV-related deregulations, like down-regulation of cell adhesion molecules and accumulation of nuclear β-catenin, which has been shown for tonsillar carcinomas and probably support successful outgrowth of tumor cells with CSC properties despite their relatively low abundance compared to HPV-unrelated primary tumors [92].

Since ALDH1$^+$ CSC might play an important role in the progression of malignancies, our findings may help to explain the better survival of HPV$^+$ OSCC patients. At this point it is

undeniable that simply enumerating the frequency of CSC populations in HR-HPV-related OSCC (low in primary and high in metastases) does not yield a satisfactory answer. However, from a genetic and developmental perspective, the CSC hypothesis may offer explanations for the different biology of tumor subgroups. It is not clear if CSC originate from the transformation of normal stem cells or also arise from restricted progenitors or differentiated cells that have re-acquired self-renewal properties as a consequence of genetic or epigenetic alterations. HPV infection regulates the basal epithelium stem cell gene expression that may lead to genetic and epigenetic changes which result in malignant phenotypes [39,43,83]. It is interesting to speculate whether the CSC will be formed from the HPV-tagged differentiated cells or not.

The genetic analysis of HR-HPV$^+$ and HPV$^-$ HNSCC has shown that TP53 mutations, especially disruptive TP53 mutations, were not identified in any of the HR-HPV$^+$ tumors but were found in 60-80% of the HPV$^-$ tumors. In an exome sequencing study of HNSCC, more genes - including TP53 and Notch, a regulator of stem and progenitor cells - were mutated per tumor in the HPV$^-$ tumors as compared to HPV$^+$ tumors [1,94]. Clinical evidence demonstrated that the disruptive TP53 mutation in HNSCC tumors predicts for loco-regional recurrence and bad survival. TP53 can also influence cellular reactive oxygen species (ROS) levels and oxidative stress by regulating the expression of pro- or anti-oxidant genes that can in turn decrease ROS levels [58]. ROS production can also be a downstream effect of p53 activation. Skinner et al. found that there was little or no ROS induction together with lack of apoptosis in disruptive TP53 mutated HNSCC tumor cells after radiation. The function and regulation of ROS in normal stem cells, which reside in niches characterized by low ROS, is a critical factor in maintaining stem cell properties such as self-renewal. There may be a crosstalk between TP53 mutation and ROS signaling pathways in the initiation and maintenance of normal stem cells and also of CSC in HPV$^-$ OSCC [25]. It is also well known that the Notch signaling pathway mainly targets programs of stem and progenitor cell differentiation [57]. In this way, the Notch mutations might influence the CSC in HPV$^-$ OSCC. As such, CSC may also become genetically unstable. It will be of future interest to elucidate HPV function in CSC together with studying genetic and epigenetic changes in OSCC.

4.5 Conclusion

In this study we characterized the patterns of ALDH1 and p16^{INK4a} expression as well as HPV infection status in primary OSCC and their corresponding lymph node metastases and correlated

the data with clinico-pathologic patient data. Our data imply that not only simply enumerating but also studying phenotypical and functional states of CSC are important to understand their specific abilities that determine differences in HPV-related and unrelated OSCC. These insights may support therapeutic design and decisions in the future.

5 References

1. Agrawal N, Frederick MJ, Pickering CR, et al. Exome sequencing of head and neck squamous cell carcinoma reveals inactivating mutations in NOTCH1. Science 2011; 333: 1154-1157.

2. Albers AE, Chen C, Koberle B, et al. Stem cells in squamous head and neck cancer. Crit Rev Oncol Hematol 2012; 81: 224-240.

3. Albers AE, Kaufmann AM. Therapeutic human papillomavirus vaccination. Public Health Genomics 2009; 12: 331-342.

4. Ang KK, Harris J, Wheeler R, et al. Human papillomavirus and survival of patients with oropharyngeal cancer. N Engl J Med 2010; 363: 24-35.

5. Anisimova E, Bartak P, Vlcek D, et al. Presence and type specificity of papillomavirus antibodies demonstrable by immunoelectron microscopy tests in samples from patients with warts. J Gen Virol 1990; 71 (Pt 2): 419-422.

6. Cardesa A, Slootweg PJ. eds. Pathology of the Head and Neck. 1th ed. Heidelberg, Germany: Springer-Verlag press, 2006: 14.

7. Arbyn M, Sanjose SD, Saraiya M, et al. EUROGIN 2011 roadmap on prevention and treatment of HPV-related disease. Int J Cancer 2012; 131: 1969-82.

8. Begum S, Westra WH. Basaloid squamous cell carcinoma of the head and neck is a mixed variant that can be further resolved by HPV status. Am J Surg Pathol 2008; 32: 1044-1050.

9. Campisi G, Giovannelli L, Calvino F, et al. HPV infection in relation to OSCC histological grading and TNM stage. Evaluation by traditional statistics and fuzzy logic model. Oral Oncol 2006; 42: 638-645.

10. Campos MS, Neiva KG, Meyers KA, et al. Endothelial derived factors inhibit anoikis of head and neck cancer stem cells. Oral Oncol 2012; 48: 26-32.

11. Chaffer CL, Weinberg RA. A perspective on cancer cell metastasis. Science 2011; 331: 1559-1564.

12. Chan PK, Yu MM, Cheung TH, et al. Detection and quantitation of human papillomavirus DNA in primary tumour and lymph nodes of patients with early stage cervical carcinoma. J Clin Virol 2005; 33: 201-205.

13. Charafe-Jauffret E, Ginestier C, Iovino F, et al. Breast cancer cell lines contain functional cancer stem cells with metastatic capacity and a distinct molecular signature. Cancer Res 2009; 69: 1302-1313.

14. Chaturvedi AK, Engels EA, Pfeiffer RM, et al. Human papillomavirus and rising oropharyngeal cancer incidence in the United States. J Clin Oncol 2011; 29: 4294-4301.

15. Chen C, Wei Y, Hummel M, et al. Evidence for epithelial-mesenchymal transition in cancer stem cells of head and neck squamous cell carcinoma. PLoS One 2011; 6: e16466.

16. Chen C, Zimmermann M, Tinhofer-Keilholz I, et al. Epithelial-to-Mesenchymal Transition and Cancer Stem(-like) Cells in Head and Neck Squamous Cell Carcinoma. Cancer Lett 2012; DOI: 10.1016/j.canlet.2012.06.013.

17. Chen YC, Chang CJ, Hsu HS, et al. Inhibition of tumorigenicity and enhancement of radiochemosensitivity in head and neck squamous cell cancer-derived ALDH1-positive cells by knockdown of Bmi-1. Oral Oncol 2010; 46: 158-165.

18. Chen YC, Chen YW, Hsu HS, et al. Aldehyde dehydrogenase 1 is a putative marker for cancer stem cells in head and neck squamous cancer. Biochem Biophys Res Commun 2009; 385: 307-313.

19. Chiou SH, Yu CC, Huang CY, et al. Positive correlations of Oct-4 and Nanog in oral cancer stem-like cells and high-grade oral squamous cell carcinoma. Clin Cancer Res 2008; 14: 4085-4095.

20. Clay MR, Tabor M, Owen JH, et al. Single-marker identification of head and neck squamous cell carcinoma cancer stem cells with aldehyde dehydrogenase. Head Neck 2010; 32: 1195-1201.

21. Cortes-Dericks L, Carboni GL, Schmid RA, et al. Putative cancer stem cells in malignant pleural mesothelioma show resistance to cisplatin and pemetrexed. Int J Oncol 2010; 37: 437-444.

22. Coutant C, Barranger E, Cortez A, et al. Frequency and prognostic significance of HPV DNA in sentinel lymph nodes of patients with cervical cancer. Ann Oncol 2007; 18: 1513-1517.

23. Cox MF, Scully C, Maitland N. Viruses in the aetiology of oral carcinoma? Examination of the evidence. Br J Oral Maxillofac Surg 1991; 29: 381-387.

24. Dahlstrom KR, Adler-Storthz K, Etzel CJ, et al. Human papillomavirus type 16 infection and squamous cell carcinoma of the head and neck in never-smokers: a matched pair analysis. Clin Cancer Res 2003; 9: 2620-2626.

25. Diehn M, Cho RW, Lobo NA, et al. Association of reactive oxygen species levels and radioresistance in cancer stem cells. Nature 2009; 458: 780-783.

26. Driessens G, Beck B, Caauwe A, et al. Defining the mode of tumour growth by clonal analysis. Nature 2012; 488: 527-530.

27. Edge SB, Byrd DR, Compton CC, et al. (eds.). AJCC Cancer Staging Manual. 7th ed. New York, NY: Springer press, 2010: 41-56.

28. Fakhry C, Westra WH, Li S, et al. Improved survival of patients with human papillomavirus-positive head and neck squamous cell carcinoma in a prospective clinical trial. J Natl Cancer Inst 2008; 100: 261-269.

29. Floor S, van Staveren WC, Larsimont D, et al. Cancer cells in epithelial-to-mesenchymal transition and tumor-propagating-cancer stem cells: distinct, overlapping or same populations. Oncogene 2011; 30: 4609-4621.

30. Gillison ML, Koch WM, Capone RB, et al. Evidence for a causal association between human papillomavirus and a subset of head and neck cancers. J Natl Cancer Inst 2000; 92: 709-720.

31. Grimm M, Krimmel M, Polligkeit J, et al. ABCB5 expression and cancer stem cell hypothesis in oral squamous cell carcinoma. Eur J Cancer 2012; 48: 3186-3197.

32. Ikenberg H. Detection of human papillomavirus DNA and RNA. In: Pfister H, ed. Prophylaxis and early detection of HPV-related neoplasia. 1th ed. Basel, Switzerland: Karger press, 2012: 109-119.

33. Pfister H. Virology and pathogenesis. In: Pfister H, ed. Prophylaxis and early detection of HPV-related neoplasia. 1th ed. Basel, Switzerland: Karger press, 2012: 1-11.

34. Hafner N, Gajda M, Altgassen C, et al. HPV16-E6 mRNA is superior to cytokeratin 19 mRNA as a molecular marker for the detection of disseminated tumour cells in sentinel lymph nodes of patients with cervical cancer by quantitative reverse-transcription PCR. Int J Cancer 2007; 120: 1842-1846.

35. Hoffmann M, Orlamunder A, Sucher J, et al. HPV16 DNA in histologically confirmed tumour-free neck lymph nodes of head and neck cancers. Anticancer Res 2006; 26: 663-670.

36. Hoffmann M, Tribius S, Quabius ES, et al. HPV DNA, E6(*)I-mRNA expression and p16(INK4A) immunohistochemistry in head and neck cancer - How valid is p16(INK4A) as surrogate marker? Cancer Lett 2012; 323: 88-96.

37. Holzinger D, Schmitt M, Dyckhoff G, et al. Viral RNA patterns and high viral load reliably define oropharynx carcinomas with active HPV16 involvement. Cancer Res 2012; 72: 4993-5003.

38. Isfoss BL, Holmqvist B, Alm P, et al. Distribution of aldehyde dehydrogenase 1-positive stem cells in benign mammary tissue from women with and without breast cancer. Histopathology 2012; 60: 617-633.

39.   Jithesh PV, Risk JM, Schache AG, et al. The epigenetic landscape of oral squamous cell carcinoma. Br J Cancer 2013; 108: 370-379.

40.   Klussmann JP, Wagner S, Wittekindt C. Tonsillar Cacer. In: Pfister H, ed. Prophylaxis and early detection of HPV-related neoplasia. 1th ed. Basel, Switzerland: Karger press, 2012: 79-85.

41.   Klingenberg B, Hafkamp HC, Haesevoets A, et al. p16 INK4A overexpression is frequently detected in tumour-free tonsil tissue without association with HPV. Histopathology 2010; 56: 957-967.

42.   Klussmann JP, Gultekin E, Weissenborn SJ, et al. Expression of p16 protein identifies a distinct entity of tonsillar carcinomas associated with human papillomavirus. Am J Pathol 2003; 162: 747-753.

43.   Klussmann JP, Mooren JJ, Lehnen M, et al. Genetic signatures of HPV-related and unrelated oropharyngeal carcinoma and their prognostic implications. Clin Cancer Res 2009; 15: 1779-1786.

44.   Klussmann JP, Weissenborn SJ, Wieland U, et al. Human papillomavirus-positive tonsillar carcinomas: a different tumor entity? Med Microbiol Immunol 2003; 192: 129-132.

45.   Krishnamurthy S, Dong Z, Vodopyanov D, et al. Endothelial cell-initiated signaling promotes the survival and self-renewal of cancer stem cells. Cancer Res 2010; 70: 9969-9978.

46.   Labrecque J, Bhat PV, Lacroix A. Purification and partial characterization of a rat kidney aldehyde dehydrogenase that oxidizes retinal to retinoic acid. Biochem Cell Biol 1993; 71: 85-89.

47.   Lapidot T, Sirard C, Vormoor J, et al. A cell initiating human acute myeloid leukaemia after transplantation into SCID mice. Nature 1994; 367: 645-648.

48.   Lassen P, Eriksen JG, Hamilton-Dutoit S, et al. Effect of HPV-associated p16INK4A expression on response to radiotherapy and survival in squamous cell carcinoma of the head and neck. J Clin Oncol 2009; 27: 1992-1998.

49.   Lee YS, Rhim CC, Lee HN, et al. HPV status in sentinel nodes might be a prognostic factor in cervical cancer. Gynecol Oncol 2007; 105: 351-357.

50.   Leemans CR, Braakhuis BJ, Brakenhoff RH. The molecular biology of head and neck cancer. Nat Rev Cancer 2011; 11: 9-22.

51.   Lewis JS Jr. p16 Immunohistochemistry as a standalone test for risk stratification in oropharyngeal squamous cell carcinoma. Head Neck Pathol 2012; Suppl 1: S75-S82.

52.   Liang C, Marsit CJ, McClean MD, et al. Biomarkers of HPV in head and neck squamous cell carcinoma. Cancer Res 2012; 72: 5004-5013.

53.   Licitra L, Perrone F, Bossi P, et al. High-risk human papillomavirus affects prognosis in patients with surgically treated oropharyngeal squamous cell carcinoma. J Clin Oncol 2006; 24: 5630-5636.

54.   Licitra L, Zigon G, Gatta G, et al. Human papillomavirus in HNSCC: a European epidemiologic perspective. Hematol Oncol Clin North Am 2008; 22: 1143-1153.

55.   Liggett WH, Jr., Sidransky D. Role of the p16 tumor suppressor gene in cancer. J Clin Oncol 1998; 16: 1197-1206.

56.   Lobo NA, Shimono Y, Qian D, et al. The biology of cancer stem cells. Annu Rev Cell Dev Biol 2007; 23: 675-699.

57.   Lobry C, Oh P, Aifantis I. Oncogenic and tumor suppressor functions of Notch in cancer: it's NOTCH what you think. J Exp Med 2011; 208: 1931-1935.

58.   Maillet A, Pervaiz S. Redox regulation of p53, redox effectors regulated by p53: a subtle balance. Antioxid Redox Signal 2012; 16: 1285-1294.

59.   Malanchi I, Santamaria-Martinez A, Susanto E, et al. Interactions between cancer stem cells and their niche govern metastatic colonization. Nature 2012; 481: 85-89.

60.   Mani SA, Guo W, Liao MJ, et al. The epithelial-mesenchymal transition generates cells with properties of stem cells. Cell 2008; 133: 704-715.

61.   Marur S, D'Souza G, Westra WH, et al. HPV-associated head and neck cancer: a virus-related cancer epidemic. Lancet Oncol 2010; 11: 781-789.

62.   Mehanna H, Beech T, Nicholson T, et al. Prevalence of human papillomavirus in oropharyngeal and nonoropharyngeal head and neck cancer-systematic review and meta-analysis of trends by time and region. Head Neck 2012; DOI: 10.1002/hed.22015.

63.   Mendelsohn AH, Lai CK, Shintaku IP, et al. Histopathologic findings of HPV and p16 positive HNSCC. Laryngoscope 2010; 120: 1788-1794.

64.   Mirghani H, Moreau F, Lefevre M, et al. Human papillomavirus type 16 oropharyngeal cancers in lymph nodes as a marker of metastases. Arch Otolaryngol Head Neck Surg 2011; 137: 910-914.

65.   Morrison SJ, Kimble J. Asymmetric and symmetric stem-cell divisions in development and cancer. Nature 2006; 441: 1068-1074.

66.   Nasman A, Attner P, Hammarstedt L, et al. Incidence of human papillomavirus (HPV) positive tonsillar carcinoma in Stockholm, Sweden: an epidemic of viral-induced carcinoma? Int J Cancer 2009; 125: 362-366.

67. Nguyen LV, Vanner R, Dirks P, et al. Cancer stem cells: an evolving concept. Nat Rev Cancer 2012; 12: 133-143.

68. Nogami T, Shien T, Tanaka T, et al. Expression of ALDH1 in axillary lymph node metastases is a prognostic factor of poor clinical outcome in breast cancer patients with 1-3 lymph node metastases. Breast Cancer 2012; DOI: 10.1007/s12282-012-0350-5.

69. Okamoto A, Chikamatsu K, Sakakura K, et al. Expansion and characterization of cancer stem-like cells in squamous cell carcinoma of the head and neck. Oral Oncol 2009; 45: 633-639.

70. Pang R, Law WL, Chu AC, et al. A subpopulation of CD26+ cancer stem cells with metastatic capacity in human colorectal cancer. Cell Stem Cell 2010; 6: 603-615.

71. Preuss SF, Klussmann JP, Semrau R, et al. Update on HPV-induced oropharyngeal cancer. HNO 2011; 59: 1031-1037.

72. Prince ME, Sivanandan R, Kaczorowski A, et al. Identification of a subpopulation of cells with cancer stem cell properties in head and neck squamous cell carcinoma. Proc Natl Acad Sci U S A 2007; 104: 973-978.

73. R V. Die cellularpathologie in ihrer begrundung auf hysiologische und pathologische gewebelehre Berlin: August Hirschwald. 1858.

74. Rampias T, Boutati E, Pectasides E, et al. Activation of Wnt signaling pathway by human papillomavirus E6 and E7 oncogenes in HPV16-positive oropharyngeal squamous carcinoma cells. Mol Cancer Res 2010; 8: 433-443.

75. Ramqvist T, Dalianis T. Oropharyngeal cancer epidemic and human papillomavirus. Emerg Infect Dis 2010; 16: 1671-1677.

76. Ramqvist T, Dalianis T. An epidemic of oropharyngeal squamous cell carcinoma (OSCC) due to human papillomavirus (HPV) infection and aspects of treatment and prevention. Anticancer Res 2011; 31: 1515-1519.

77. Reimers N, Kasper HU, Weissenborn SJ, et al. Combined analysis of HPV-DNA, p16 and EGFR expression to predict prognosis in oropharyngeal cancer. Int J Cancer 2007; 120: 1731-1738.

78. Rischin D, Young RJ, Fisher R, et al. Prognostic significance of p16INK4A and human papillomavirus in patients with oropharyngeal cancer treated on TROG 02.02 phase III trial. J Clin Oncol; 28: 4142-4148.

79. Riveros-Rosas H, Julian-Sanchez A, Pina E. Enzymology of ethanol and acetaldehyde metabolism in mammals. Arch Med Res 1997; 28: 453-471.

80. Robinson M, Sloan P, Shaw R. Refining the diagnosis of oropharyngeal squamous cell carcinoma using human papillomavirus testing. Oral Oncol 2010; 46: 492-496.

81. Russo JE, Hilton J. Characterization of cytosolic aldehyde dehydrogenase from cyclophosphamide resistant L1210 cells. Cancer Res 1988; 48: 2963-2968.

82. Sarrio D, Franklin CK, Mackay A, et al. Epithelial and mesenchymal subpopulations within normal basal breast cell lines exhibit distinct stem cell/progenitor properties. Stem Cells 2012; 30: 292-303.

83. Sartor MA, Dolinoy DC, Jones TR, et al. Genome-wide methylation and expression differences in HPV(+) and HPV(-) squamous cell carcinoma cell lines are consistent with divergent mechanisms of carcinogenesis. Epigenetics 2011; 6: 777-787.

84. Schache AG, Liloglou T, Risk JM, et al. Evaluation of human papilloma virus diagnostic testing in oropharyngeal squamous cell carcinoma: sensitivity, specificity, and prognostic discrimination. Clin Cancer Res 2011; 17: 6262-6271.

85. Schache AG, Liloglou T, Risk JM, et al. Validation of a novel diagnostic standard in HPV-positive oropharyngeal squamous cell carcinoma. Br J Cancer 2013; DOI: 10.1038/bjc.2013.63.

86. Schiller JT, Day PM, Kines RC. Current understanding of the mechanism of HPV infection. Gynecol Oncol 2010; 118: S12-17.

87. Settle K, Posner MR, Schumaker LM, et al. Racial survival disparity in head and neck cancer results from low prevalence of human papillomavirus infection in black oropharyngeal cancer patients. Cancer Prev Res (Phila) 2009; 2: 776-781.

88. Singh A, Settleman J. EMT, cancer stem cells and drug resistance: an emerging axis of evil in the war on cancer. Oncogene 2010; 29: 4741-4751.

89. Sladek NE. Human aldehyde dehydrogenases: potential pathological, pharmacological, and toxicological impact. J Biochem Mol Toxicol 2003; 17: 7-23.

90. Smeets SJ, Hesselink AT, Speel EJ, et al. A novel algorithm for reliable detection of human papillomavirus in paraffin embedded head and neck cancer specimen. Int J Cancer 2007; 121: 2465-2472.

91. Smith EM, Wang D, Kim Y, et al. P16INK4a expression, human papillomavirus, and survival in head and neck cancer. Oral Oncol 2008; 44: 133-142.

92. Stenner M, Yosef B, Huebbers CU, et al. Nuclear translocation of beta-catenin and decreased expression of epithelial cadherin in human papillomavirus-positive tonsillar cancer: an early event in human papillomavirus-related tumour progression? Histopathology 2011; 58: 1117-1126.

93.   Stone S, Jiang P, Dayananth P, et al. Complex structure and regulation of the P16 (MTS1) locus. Cancer Res 1995; 55: 2988-2994.

94.   Stransky N, Egloff AM, Tward AD, et al. The mutational landscape of head and neck squamous cell carcinoma. Science 2011; 333: 1157-1160.

95.   Syrjanen K, Syrjanen S, Lamberg M, et al. Morphological and immunohistochemical evidence suggesting human papillomavirus (HPV) involvement in oral squamous cell carcinogenesis. Int J Oral Surg 1983; 12: 418-424.

96.   Tribius S, Ihloff AS, Rieckmann T, et al. Impact of HPV status on treatment of squamous cell cancer of the oropharynx: what we know and what we need to know. Cancer Lett 2011; 304: 71-79.

97.   Visvader JE, Lindeman GJ. Cancer stem cells in solid tumours: accumulating evidence and unresolved questions. Nat Rev Cancer 2008; 8: 755-768.

98.   Wang F, Flanagan J, Su N, et al. RNAscope: a novel in situ RNA analysis platform for formalin-fixed, paraffin-embedded tissues. J Mol Diagn 2012; 14: 22-29.

99.   Wang R, Chadalavada K, Wilshire J, et al. Glioblastoma stem-like cells give rise to tumour endothelium. Nature 2010; 468: 829-833.

100. Warnakulasuriya S. Global epidemiology of oral and oropharyngeal cancer. Oral Oncol 2009; 45: 309-316 .

101. Xu J, Muller S, Nannapaneni S, et al. Comparison of quantum dot technology with conventional immunohistochemistry in examining aldehyde dehydrogenase 1A1 as a potential biomarker for lymph node metastasis of head and neck cancer. Eur J Cancer 2012; 48: 1682-91.

102. Yang WH, Lan HY, Huang CH, et al. RAC1 activation mediates Twist1-induced cancer cell migration. Nat Cell Biol 2012; 14: 366-374.

103. Zhang Q, Shi S, Yen Y, et al. A subpopulation of CD133(+) cancer stem-like cells characterized in human oral squamous cell carcinoma confer resistance to chemotherapy. Cancer Lett 2010; 289: 151-160.

104. zur Hausen H. Papillomaviruses and cancer: from basic studies to clinical application. Nat Rev Cancer 2002; 2: 342-350.

6 Affidavit

"I, [XU, QIAN] certify under penalty of perjury by my own signature that I have submitted the thesis on the topic [ALDH1-positive cancer stem-like cells enrich in nodal metastases of oropharyngeal squamous cell carcinoma independently of HPV-status] I wrote this thesis independently and without assistance from third parties, I used no other aids than the listed sources and resources.

All points based literally or in spirit on publications or presentations of other authors are, as such, in proper citations (see "uniform requirements for manuscripts (URM)" the ICMJE www.icmje.org) indicated. The sections on methodology (in particular practical work, laboratory requirements, statistical processing) and results (in particular images, graphics and tables) correspond to the URM (s.o) and are answered by me. My interests in any publications to this dissertation correspond to those that are specified in the following joint declaration with the responsible person and supervisor. All publications resulting from this thesis and which I am author correspond to the URM (see above) and I am solely responsible.

The importance of this affidavit and the criminal consequences of a false affidavit (section 156,161 of the Criminal Code) are known to me and I understand the rights and responsibilities stated therein.

Date   Signature

<u>Declaration of any eventual publications</u>

 [XU QIAN] had the following share in the following publications:

Publication 1: [**Qian X**, Wagner S, Ma C, Klussmann JP, Hummel M, Kaufmann AM, Albers AE], [ALDH1-positive cancer stem-like cells enrich in nodal metastases of oropharyngeal squamous cell carcinoma independent of HPV-status], [Oncol Rep], [2013]
Contribution in detail (please briefly explain): Qian X performed the experiments, analysed the data, and wrote the paper.

Publication 2: [Liao T, Kaufmann AM, **Qian X**, Sangvatanakul V, Zhang G, Albers AE], [Susceptibility to cytotoxic T cell lysis of cancer stem cells derived from cervical and head and neck tumor cell lines], [J Cancer Res Clin Oncol], [2013]

Contribution in detail (please briefly explain): Qian X contributed to the cancer stem-like cells culture and data analysis in part.

Publication 3: [Niebler M, **Qian X**, Höfler D, Kogosov V, Kaewprag J, Kaufmann AM, Ly R, Böhmer G, Zawatzky R, Rösl F, Rincon-Orozco B], [Post-translational control of IL-1β via the human papillomavirus type 16 E6 oncoprotein: anovel mechanism of innate immune escape mediated by the E3-ubiquitin ligase E6-AP and p53], [Plos Pathegen], [2013]

Contribution in detail (please briefly explain):

Qian X participated in the performance of the experiments and data analysis.

Signature, date and stamp of the supervising University teacher

_____

Signature of the doctoral candidate

_____

7 Curriculum vitae and publications

Mein Lebenslauf wird aus datenschutzrechtlichen Gründen in der elektronischen Version meiner Arbeit nicht veröffentlicht.

Publications:

1. **Qian X**, Wagner S, Ma C, Klussmann JP, Hummel M, Kaufmann AM, Albers AE. ALDH1-positive cancer stem-like cells enrich in nodal metastases of oropharyngeal squamous cell carcinoma independent of HPV-status. *Oncol Rep*. 2013. 29:1777-1784.

2. **Qian X**, Ma C, Nie X, Lu J, Kaufmann AM, Albers AE. Targeting cancer stem(-like) cells in head and neck cancer: from an immunotherapy perspective. *Crit Rev Oncol Hematol*. Under review.

3. Niebler M, **Qian X**, Höfler D, Kogosov V, Kaewprag J, Kaufmann AM, Ly R, Böhmer G, Zawatzky R, Rösl F, Rincon-Orozco B. Post-translational control of IL-1β via the human papillomavirus type 16 E6 oncoprotein: a novel mechanism of innate immune escape mediated by the E3-ubiquitin ligase E6-AP and p53. *Plos Pathegen*. 2013. 9:e1003536.

4. Liao T, Kaufmann AM, **Qian X**, Sangvatanakul V, Zhang G, Albers AE. Susceptibility to cytotoxic T cell lysis of cancer stem cells derived from cervical and head and neck tumor cell lines. *J Cancer Res Clin Oncol*. 2013. 139:159-170.

5. Ren Y, Yang S, Tan G, Ye W, Liu D, **Qian X**, Ding Z, Zhong Y, Zhang J, Jiang D, Zhao Y, Lu J. Reduction of mitoferrin results in abnormal development and extended lifespan in caenorhabditis elegans. *Plos one*. 2012. 7: e29666.

6. Albers AE, Chen C, Koberle B, **Qian X**, Klussmann JP, Wollenberg B, Kaufmann AM. Stem cells in squamous head and neck cancer. *Crit Rev Oncol Hematol*. 2012. 81:224-40.

7. **Qian X**, Zhang C, Zhang J, Ren Y, Lei Y. Changes of acetylcholine and carbon monoxide producing neurons in colon of scalded rat during early post-burn stage. *J of Wenzhou Medical College*. 2009.36:122-124. In Chinese.

8. Ye S, Su ZP, Zhang J, **Qian X**, Zhuge QC, Zheng YJ. Differential centrifugation in culture and differentiation of rat neural stem cells. *Cell Mol Neurobiol*. 2008. 28: 511-517.

9. Lei Y, Dong Y, **Qian X**. Delayed gastrointestinal transit time and changes of ileum myenteric plexue in diabetic rats. *Chinese J of Digestion*. 2006.26:666-669. In Chinese.

10. Ye S, Su ZP, **Qian X**, Zhuge QC. Culture and identification of embryonic rat neural stem cells in vitro. *J of Wenzhou Medical College*. 2005.35:449-451. In Chinese.

Book Chapters

1. **Qian X**, Kaufmann AM, Albers AE. Immunopathology of head and neck tumors and immunotherapy of squamous cell carcinoma. In: Rezaei N, ed. 2013, Springer Science press. Accepted and unpublished.

2. Zimmermann M, **Qian X**, Kaufmann AM, Albers AE. The role of cancer stem(-like) cells and epithelial-to-mesenchymal transition in spreading head and neck Squamous Cell Carcinoma. In: Hayat MA, ed. Stem Cells and Cancer Stem Cells. Springer Science press. 2013, Volume 11, DOI:10.1007/978-94-007-7329-5_6.

3. **Qian X**, Kaufmann AM, Albers AE. Cancer stem cells of the head and neck. In: Hayat MA, ed. Stem Cells and Cancer Stem Cells. Springer Science press. 2012:275-286. Online ISBN 978-94-007-4798-2, print ISBN 978-94-007-4797-5.

Conference abstracts

1. **Qian X**, Kaufmann AM, Albers AE. Phenotype of p53 wild-type epitope specific T cells in the circulation of patients with head and neck cancer. *8th PhD-Symposium – "Bringing Future Scientists Together"& DRS presentation seminar*. Oral presentation. Jul 2013, Freie University Berlin, Germany.

2. **Qian X**, Ma C, Hummel M, Wagner S, Klussmann JP, Kaufmann AM, Albers AE. ALDH1-positive cancer stem-like cells are associated with HR-HPV-expression in oropharyngeal squamous cell carcinoma and nodal metastases. International conference on "Emerging Concepts in Cancer". Poster exhibition. Jun. 2012, Berlin, Germany.

2. **Qian X**, Hummel M, Wagner S, Klussmann JP, Kaufmann AM, Albers AE. ALDH1-positive cancer stem cells are associated with HR-HPV+/p16+ expression in HNSCC. 27th International Papillomavirus Conference and Clinical Workshop. Poster exhibition. Sept. 2011, Berlin, Germany.

8 Acknowledgements

Time flies away. At this moment, memory takes me back to the very first day when I gave my oath to be a medical student. I still remembered one of my supervisors said to us, "From now on, you'll be on a journey between who you think you are and who you can be." Now, I am still on this journey to dream my dream and pursue my career.

Three years study at Charité, it cultivate my ability to develop the passion for assimilating modern thinking and applying it to the understanding of the disease on different levels. Today, we live in a world in prosperity but are still threatened by so many problems. Failure for the cancer treatment is an appalling fact. Cancer stem-like cells, a promising field of therapy targets, give us a hope.

When I wrote my thesis in Berlin, I heard the bad news from my father. He had a surgery due to gastric adenocarcinoma. I typed these words with tears, but it strengthened my determination to devote my whole life to this journey. It is with those peoples' spirit, passion, courage and strong sense, we are taking our steps with efforts into the world. And I am pretty sure, no matter who we are, what we do and where we go, we will fight for it ever and finally conquer it.

Finally, I would like to thank all the people who taught me, nurtured me, helped me and gave me a hand always. My supervisors, Dr. Kaufmann and Dr. Albers, Prof. Hummel and Ms. Berg of Institute of Pathology, Prof. Klussmann and Dr. Wagner from Giessen, Ms. Glowacki and Ms. Helmke of Charité welcome center, laboratory members, Ms. Noske-Reimers, Dr. Kube. Other Dr. Med candidates, Dr. Wang, Dr. Liao, Dr. Luo, Dr. Ma, Dr. Zhang, Dr. Xia, and those kind persons I even didn't know the name.

Thank you, all my family members, who understand and support me for a long time leaving home. Despite of talking every day, I still miss so much.

Good luck, papa!
Thank you, Charité!
Thank you, Germany!